

Copyright Warning & Restrictions

The copyright law of the United States (Title 17, United States Code) governs the making of photocopies or other reproductions of copyrighted material.

Under certain conditions specified in the law, libraries and archives are authorized to furnish a photocopy or other reproduction. One of these specified conditions is that the photocopy or reproduction is not to be “used for any purpose other than private study, scholarship, or research.” If a user makes a request for, or later uses, a photocopy or reproduction for purposes in excess of “fair use” that user may be liable for copyright infringement,

This institution reserves the right to refuse to accept a copying order if, in its judgment, fulfillment of the order would involve violation of copyright law.

Please Note: The author retains the copyright while the New Jersey Institute of Technology reserves the right to distribute this thesis or dissertation

Printing note: If you do not wish to print this page, then select “Pages from: first page # to: last page #” on the print dialog screen

The Van Houten library has removed some of the personal information and all signatures from the approval page and biographical sketches of theses and dissertations in order to protect the identity of NJIT graduates and faculty.

Burn Wound Healing Evaluation By Infrared Imaging

by
Shang-Yuan Chen

Thesis submitted to the Faculty of the Graduate School of
the New Jersey Institute of Technology in partial fulfillment of
the requirements for the degree of
Master of Science in Biomedical Engineering
1991

Approval Sheet

Title of Thesis: Burn Wound Healing Evaluation By Infrared Imaging

Name of Candidate: Shang-Yuan Chen

Master of Science in Biomedical Engineering

Thesis and Abstract Approved: _____

Dr. Peter Engler

Date 1-92

Department of Electrical and Computer Engineering,

NJIT, Newark, N.J.

Dr. Arthur B. Ritter

Date 1-92

Department of Physiology,

UMDNJ-New Jersey Medical School, Newark, N.J.

Dr. David Kristol

Date 1-92

Department of Biomedical Engineering, NJIT, Newark, N.J.

VITA

Name: Shang-Yuan Chen

Degree and date to be conferred: Master of Science in
Biomedical Engineering Jan. 1992

<u>Collegiate institutions attended</u>	<u>Dates</u>	<u>Degree</u>
Taiwan Fu-Jen Catholic University	9/82 - 6/86	B.S.(Physics)
New Jersey Institute of Technology	1/90 - 1/92	M.S.(Biomedical Engineering)

To my wife, Annie, and my parents

Acknowledgement

I am deeply indebted to my primary thesis advisor Dr. Peter Eagler for his expert guidance and assistance. His constant encouragement and thoroughness contributed toward the completion of this thesis. Special thanks are also due to my other advisors, Dr. David Kristol and Dr. Arthur B. Ritter, for their advice, support and encouragement. Mr. Mehul M. Patel provided technical support towards the operation of the IR-imaging system at the Saint Barnabas Medical Center Burn Unit, Livingston, N.J, and Dr. Julian P. Keogh provided valuable assistance towards the final preparation of this thesis. Finally, I would like to thank my friends Mr. Gung-Wei Chirn, Mr. Yui-Liang Chen and Dr. Liu Jing for their valuable support, assistance and patience during the months which went into the production of this document.

Abstract

Title of Thesis: **Burn Wound Healing Evaluation By**

Infrared Imaging

Shang-Yuan Chen, Master of Science in Biomedical Engineering, 1991.

Thesis directed by: Dr. Peter Engler

Department of Electrical and Computer Engineering, NJIT,
Newark, N.J.

Dr. Arthur B. Ritter

Department of Pysiology,

UMDNJ-New Jersey Medical School, Newark, N.J.

Dr. David Kristol

Department of Biomedical Engineering, NJIT, Newark, N.J.

Infrared imaging is a pictorial method of temperature representation. Its advantage in the treatment of burns is that it is a non-invasive, safe and reliable method for estimating the area, temperature and depth of burns. An Imaging Burn program was developed for comparing changes in burn area in response to treatment with time. The program proved itself capable of determining the surface area of simulated lesions on the skin of human volunteers to within an error of 1.6 percent. The size and temperature of burn lesions in patients was recorded. First degree burns were warmer than surrounding areas of normal skin, whereas second degree burns were colder, and

third degree burns colder still. The technique and program as presented may prove a valuable supplement to clinical examination for burn diagnosis and monitoring.

Contents

1	INTRODUCTION	1
1.1	Background	1
1.2	Burn area estimation	2
1.3	Burn depth estimation - thermography	7
1.4	The Infrared (IR) Camera	9
1.5	Aims of current study	13
2	METHODS	14
3	THEORY	20
3.1	Temperature	20
3.2	Imaging processing	23
3.2.1	Thresholding	24
3.2.2	Noise removal	25
3.2.3	Boundary retrieving	26
3.2.4	Area calculation	29

3.2.5	Finding major axis	30
3.2.6	Geometric Transformation	31
3.2.7	Gray level interpolation	41
4	RESULT AND DISCUSSION	43
5	CONCLUSIONS	53
6	REFERENCES	76
7	APPENDIX: BURN PROGRAM	83

1 INTRODUCTION

1.1 Background

Burn injuries are the largest surface wounds treated in medicine. In 1860, Timothy Holmes [1] wrote, “These injuries have been variously classified, into four divisions by Heister and Callisen, into six by Dupuytren, and various other divisions have been proposed; all of them indicating the depth of tissue implicated in the injury. Another, and perhaps even more important, consideration is the extent of the burned surface - a matter which necessarily eludes formal classification.”

Burns are of varying severity and range from minor discomforts to those causing death. Minor burns, classified as first degree, occur at temperatures above the pain threshold and range from light to severe erythema (*i.e.* reddening of the skin caused by increased blood microcirculation). With these burns the skin returns to its normal appearance within 24 hours. Second

degree burns range in intensity from a mild burn with a few small blisters to a more severe burn involving a blister covering the entire exposed area. Second degree burns involve the discarding of injured tissue but do not involve destruction of the full thickness of the skin, and will heal to an essentially normal skin after at least a week. Third degree burns, involving at least all of the skin layers, are called “full thickness” burns and leave scars on healing unless special grafting techniques are employed [2].

1.2 Burn area estimation

An easy method to estimate the surface area of the human body has long been sought. In 1879, von Meeh developed a formula to calculate the body surface area which was based on body weight. However, although measurements which were accurate to an error of 7 percent were claimed, these estimates were largely dependent on the stature of individuals under observation [3]. In 1915, DuBois proposed a relationship for body surface area based on the

patient's height and weight [4]. The relationship is still widely used to this day. The formula is derived from a model which depicts the human body as a series of cylinders, the area of each being circumference times height. The formula, described below, is for the total body surface area of adults;

$$Body\ surface\ area = \frac{weight(kg)^{0.425} \times height(cm)^{0.725} \times 71.84}{10^4} sq.meters$$

In 1924, the importance of accurate estimations of burn area was first recognized independently by both Berkow [5] and Weidenfeld [6]. They defined procedures for burn area estimation which involved 1): actual measurement of burned surface area in specific body parts 2): calculation of the proportion of total body area present in those body parts, and 3): determination of the proportion of total body area burned by calculating the product of 1) and 2) for each area affected. The first step in Berkow's procedure was to determine mathematically the proportions of total surface area that were present in the head, trunk, upper extremities and lower extremities. Then it was determined whether there existed a constancy of these proportions in persons of

different physique. Berkow's table did indeed reveal that constancy existed between adults of widely differing physique, however, the proportions did tend to vary widely between infants, children and adults.

In 1944, Lund and Browder [7] proposed a new table based on the concepts of Weidenfeld [6], Dubois [4], and Boyd [8] which corrected for the systematic errors which can occur when, for example, Berkow's table for adults is applied to children. However, because of certain inconveniences and difficulties associated with the use of the Lund and Browder chart, Pulaski and Tennison in 1947 devised the Rule of Nines. They found that the percentage of each body segment was approximately equivalent to a multiple of nine (table 1) [9].

Region	Percentage of Total Body Area
Head and Neck	9
Upper extremities	9 (each)
Lower extremities	18 (each)
Anterior trunk	18
Posterior trunk	18
Genetalia	1

Table 1: THE RULE OF NINES

Although the accuracy of the Rule of Nines has been proven, the estimates on burn area are subject to considerable error arising from observer bias. A comparison of burn areas estimated on three simulated patients by four surgical residents is summarized in Table 2.

The Rule of Nines is one of the most commonly used methods to estimate

volunteer	Estimated burn area				area by direct direct measurement	average error	ratio average error to direct measurement
	1	2	3	4			
	%				%	%	%
A	28	25	30	36	28.5	3	10:100
B	17	17	22	19	11.9	6.9	58:100
C	27	38	35	34	30.9	4.6	15:100

Table 2: Estimation by 4 surgical residents, using the Rule of Nines to evaluate volunteers with irregular areas of their bodies outlined and assumed “burned”.

burn area. However, in many cases it is difficult to differentiate between areas of full thickness burn (third degree) and areas of deep partial thickness burn (deep second degree). The clinical accuracy of the diagnosis depends on the experience and training of the physician.

More recently in 1985, Nichter, Bryant and Edlich used computer generated human facsimiles with simulated burns, to assess the accuracy with which physicians estimate burn areas [10]. The wide variations observed, and their inconsistency with the correctly calculated values, revealed the need for a more effective procedure to determine burn area. Also, the adoption of early excision and grafting as a method of treating deep burn injuries has emphasized the requirement for an accurate and reliable procedure for measuring the depth of burn injury [11].

1.3 Burn depth estimation - thermography

Several methods for determining burn depth have been made available to physicians. They can be categorized as either invasive or non-invasive procedures. One particular measuring technique that may be of assistance in the assessment of burn depth is the non-invasive technique of thermographic imaging. Thermography is concerned with the analysis of heat distribution [12]. Specifically, it involves the graphic representation of heat patterns which is usually accomplished using computer-aided displays and photographic techniques.

Clinical thermography is a relatively new diagnostic concept. It has been known for some time that most breast cancers are characterized by an increase in temperature [13]. This heat elevation can be detected in the skin over the cancer, and, in fact, often the whole breast, if the temperature recording instrumentation is sufficiently sensitive [14]. In the 1960's this phenomenon was explored for its potential to differentiate between normal

and malignant growths both in the breast and elsewhere [15]. In the 1980's thermography for the detection of breast tumor was replaced by mammography.

The measurement of these temperature changes involves seeking out the most sophisticated infrared instrumentation as a starting point. A thermometer is an instrument for measuring temperature, whereas a thermograph is a registering thermometer or an instrument which records spatial or temporal heat distributions. Thermography, since it is based upon the use of a scanning radiometer, extends the range of noncontact pyrometry to small variations in human skin temperatures, and provides graphic representations of the temperature's distribution over the surface of the subject [13].

Thermography machines were improved and developed principally for national defense and space programs, but have since become available for, and applicable to, medical research in many fields. In 1956, Lawson observed

elevated skin temperatures over carcinoma of the breast [15] and Williams *et al.* have confirmed and extended these observations [16]. In 1961 Lawson reported on the use of thermographic studies of burns and frostbites in dogs [17].

Only the fact that adequate recording technology has recently become practical allows thermography to be considered an effective means of heat pattern description. Hackett (1974) investigated 109 burn patients and concluded that thermography as a method for diagnosing depth of burn was superior to clinical examination [18].

1.4 The Infrared (IR) Camera

The IR Camera infrared charge-coupled device Camera system (IR-CCD) consists of two units, *i.e.* the camera head, and the uniformity corrector. The camera head electronics include the timing and the driver circuits. Also

contained in this system are all the controls required for the operation of the 320×244 IR-CCD imager.

The 320×244 IR-CCD image sensor with the PtSi (Platinum silicide) Schottky-barrier detector used in this thesis was developed at the David Sarnoff Research Center (figure 1)[19].

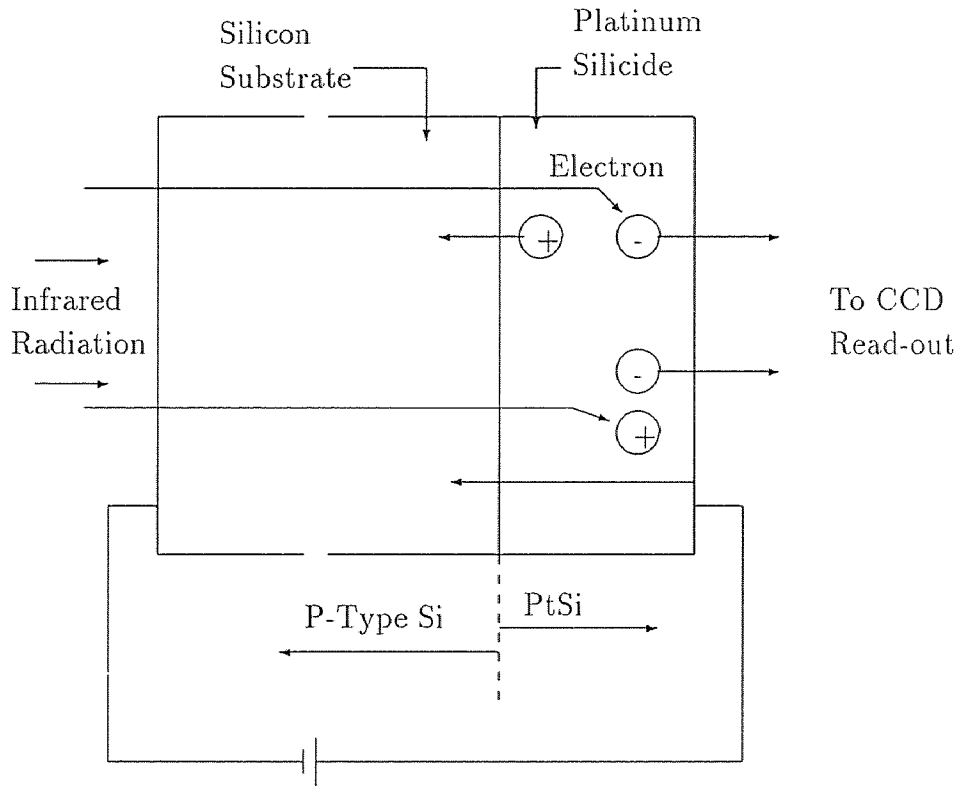


Figure 1

The IR-CCD imager is operated at about $77K$ in a liquid nitrogen dewar at 30 frames/sec with a $3.4\text{ }\mu\text{m}$ long-pass filter and f/1.4 optics. Under these conditions the imager could detect wavelengths of between 3.4 and $20\text{ }\mu\text{m}$ [22]. The infrared radiation with photon energy less than the band gap of silicon ($E_g=1.12\text{ eV}$) is transmitted through the silicon substance. The absorption of infrared radiation in the silicide layer results in the excitation of photocurrent across the Schottky-barrier by the internal photoemission. The Schottky-barrier is the barrier that is formed between the platinum silicide layer and the p-type silicon substrate.

The minimum resolvable temperature, which is a subjective measurement describing the temperature and spatial resolution of an infrared imaging system, was around $0.1^\circ C$. This was in the order of the minimum acceptable resolution for the type of studies we were performing.

The thermal imaging in the medium wavelength infrared and long wave-

length infrared bands is based on the detection of thermal radiation from a scene and corresponds to the spatial variations of temperature and emissivity. Emissivity is the ratio of radiance of the body in question to that of a theoretical black body.

The image sensors were developed for thermal imaging in the medium wavelength infrared (MWIR, 3-5 μm) and long wavelength infrared (LWIR, 8-12 μm) bands. Table 3 shows that thermal imaging can be accomplished in the MWIR and LWIR bands with the photon flux shown ($\text{photons/s} - \text{cm}^2$) and background temperature of 300K [20].

Spcetral Band	OBJECT PHOTON FLUX (photons/s/cm^2)	CONTRAST
0.4 to 0.7 μm	10^8 to 10^{17}	0.2 to 8
3 to 5 μm	1.3×10^{15}	$0.045/^{\circ}\text{C}$
8 to 12 μm	8.0×10^{16}	$0.02/^{\circ}\text{C}$

Table 3: Comparison of emitted photon flux and contrast for visible (0.4 to 0.7 μm) and infrared (3 to 5 μm and 8 to 12 μm) imaging. Contrast describes the maximum number of resolvable temperature changes per unit temperature change.

The IR-CCD image sensors exhibit two types of noise in the displayed image, a temporal noise and a spatial fixed pattern noise. The temporal noise at the output sensing node and the low frequency components of the $1/f$ noise can be substantially reduced by using correlated-double sampling at the output signal. The uniformity corrector digitally subtracts a reference frame from each video signal frame of the IR-CCD camera to substantially reduce the spatial noise in the output display.

1.5 Aims of current study

In recent years increased thought has been given to relating surface body temperature to underlying pathology and physiology. Our investigation used an improved method for estimating the depth of the burn injury utilizing infrared imaging. The image intensity was compared by eye with burn areas on the thermograph in order to determine differential temperatures.

2 METHODS

Thermal imaging has presented a major advance in the study of skin temperature. The temperature distribution of small or large areas of the body can now be recorded instantaneously and without contact with the patient. However, the thermal state is a dynamic situation, constantly changing in response to metabolic demands and the influence of the body's environment. In spite of this fact, consistent normal patterns can be identified on most of the surfaces of the body although they are more readily seen when the subject is examined under controlled environmental conditions.

The subjects that participated in this pilot study were patients in the Burn Unit at the Saint Barnabas Medical Center in Livingston, N.J. The subjects signed an "Informed Consent" form agreeing to have their injuries recorded on an infrared imaging system.

The recording was accomplished in the Tank Room of the burn unit where the injuries were washed prior to recording. The temperature of the tank room was maintained at 20°C (293K) and relative humidity controlled at between 40% and 60%. During the imaging and the subsequent wound dressing the patients were under a canopy-type heat source to keep them comfortable. It was assumed that the temperature of the burn injuries was at equilibrium.

Fig. 2 is a block diagram of the recording system, consisting of the IR camera, TV monitor and video cassette recorder.

The recorded images were subsequently processed on an image processing subsystem outlined in Fig. 3. This subsystem was located at the Physiology Department at the UMDNJ in Newark, N.J.

The analog data on the video tape was digitized on a Quantex Corp model

DS20F image digitizer. The output from the digitizer was transmitted over an HP-IB(IEEE 488) bus to a Hewlett-Packard model A-900 computer. The video frames in the digitizer could be controlled manually or by the computer.

The DS20F (Digital Image Memory) offers the capability of digitizing and storing TV images in one field or one frame time. Images digitized by the DS20F can originate from any source providing standard RS170 (e.g. video tape recorders). The unit combines a fast A/D converter and high capacity random access memory. The sample matrix is 512 x 512 (picture elements). The gray scale range was described in 8 bits per picture element (providing 256 increments in total on the gray scale range).

The digital image is first transferred into the Quantex digitizer's memory. The digitized image is processed by the HP 1000 computer and the processed image is stored on a high capacity disk (HP 7958, 10 Mbytes).

To evaluate the image processing software, rectangular aluminum plates of various known dimensions (between 6 and 21 cm^2) were attached to the arms of normal subjects. Being highly reflective, the aluminum plates could be used to simulate real burns. The aluminum model was readily imaged on the IR imaging system. Computer algorithms were written to record the temperature distribution across the arm with the aluminum plate attached, as well as an algorithm to estimate the surface area of the plate.

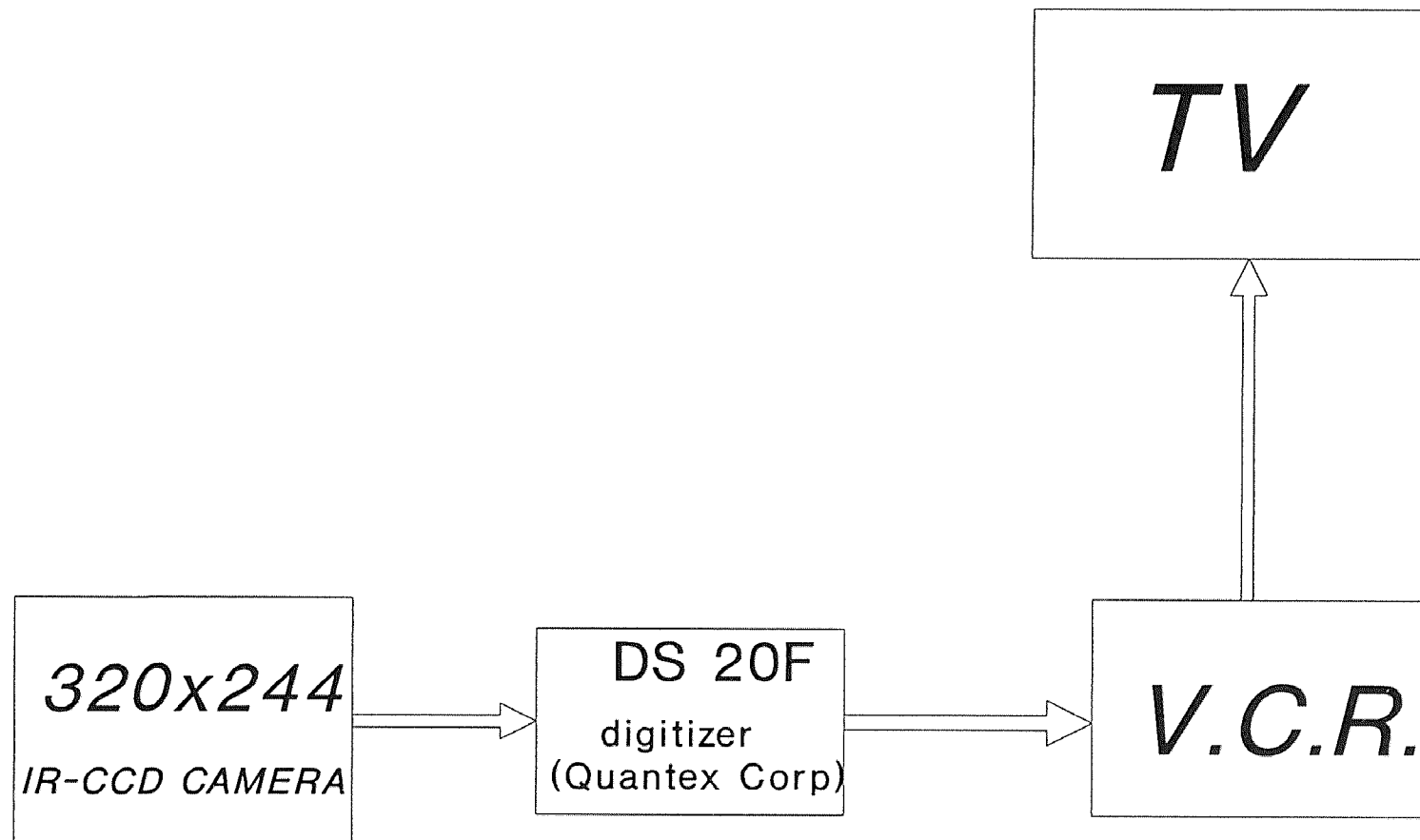


Fig 2 The image experiment system

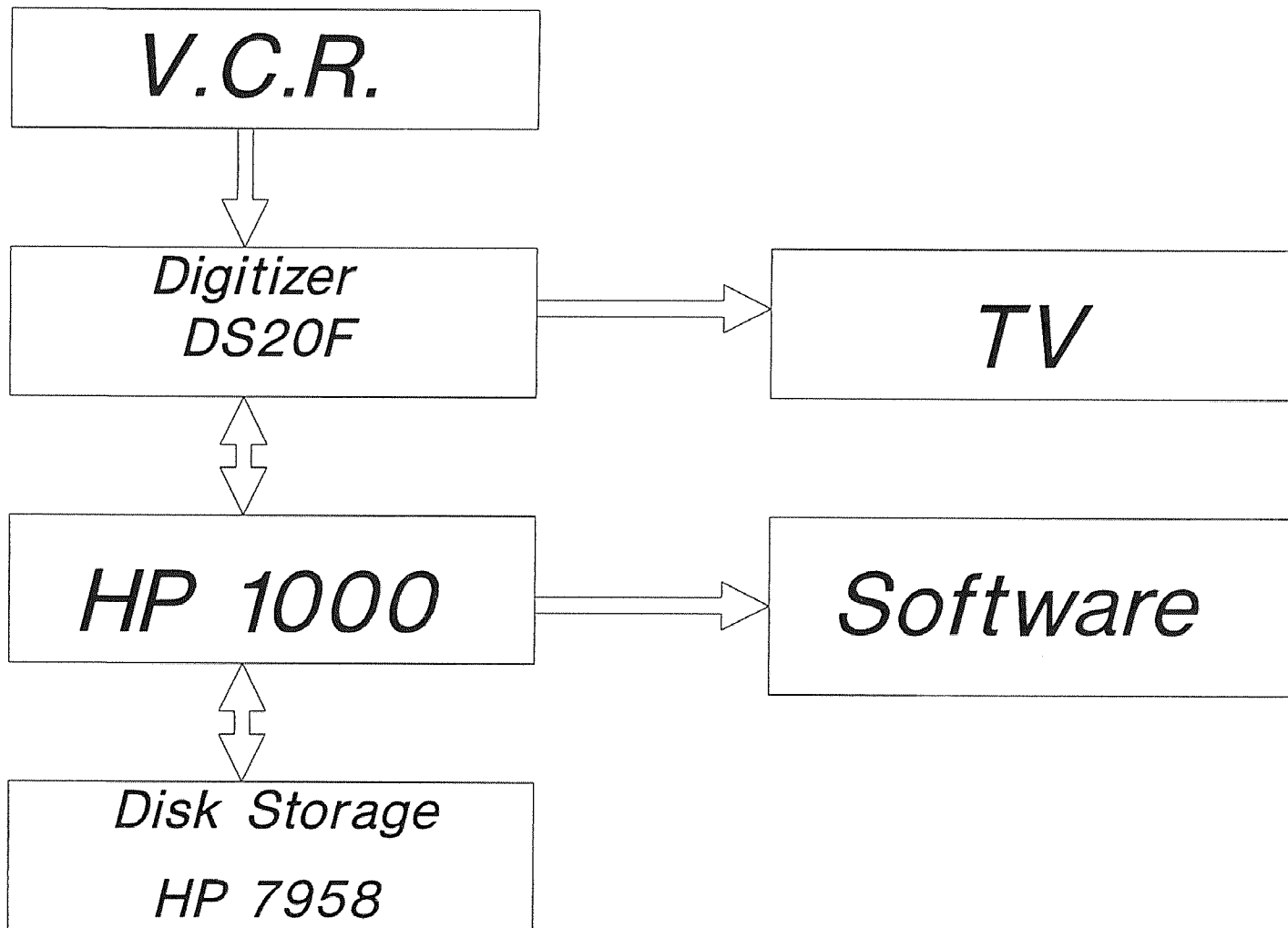


Fig 3 The image processing subsystem

3 THEORY

3.1 Temperature

In order to understand the problem which can occur in measurement of temperature, we must appreciate some of the aspects of infrared radiation from the skin. The basic Law of Max Planck in 1901 describes the power radiated per unit area per unit wavelength interval of a perfect emitter (a “black body”) as given by Planck’s function:

$$I(\epsilon, \lambda, T) = \epsilon \ c_1 \ \lambda^{-5} \{[\exp(c_2/\lambda T)] - 1\}^{-1}$$

where

$$I = \text{watt} - \text{cm}^{-2};$$

$$\epsilon = \text{emissivity};$$

$$c_1 = 3.74 * 10^{-12} \text{watt} - \text{cm}^2;$$

$$c_2 = 1.44 \text{ cm} - \text{degree};$$

$$\lambda = \text{wavelength in cm};$$

$T = \text{Temperature in } K.$

The quantity I is called the spectral radiant emittance, that is the emittance at any specific wavelength [21]. The total radiant emittance, W , is that which would be obtained across the entire electromagnetic spectrum from a perfect radiator. The radiant emittance in any spectral interval $W_{\lambda_1-\lambda_2}$ is obtained by integrating the Planck equation over the limits of the spectral range.

$W_{\lambda_1-\lambda_2} = \int_{\lambda_2}^{\lambda_1} I_{\lambda} d\lambda$ The total radiant emittance from the black body can be found by integrating I over all wavelengths.

$$W = \int_0^{\infty} I_{\lambda} d\lambda$$

$$= \epsilon \sigma T^4$$

where W is the radiant energy every emitted per unit area (watts cm^{-2}), σ is the Stefan - Boltzmann constant (5.673×10^{-8} watts $cm^{-2}K^{-4}$), and T is the surface temperature of the object expressed in degrees Kelvin. ϵ is a function of wavelength and depends upon the chemical and physical nature of the object and its surface [15]. For a theoretically perfect mirror which would reflect 100 percent of the energy which falls upon it, ϵ would be zero; for a perfectly transparent object which neither absorbs nor reflects incident energy, ϵ would also be equal to zero; for a perfect absorber, ϵ would be equal to unity, and such an object would be called a “black body”. Since σ is a constant, it follows that $W \propto \epsilon T^4$. Therefore if W can be measured and ϵ is known, T can be computed.

No perfect black body with an emissivity of unity exists. Human skin is partially transparent and partially reflective to visible light and the near infrared, but its optical properties at longer wavelengths are different. In 1939 Hardy showed that the human skin is a nearly perfect absorber and emitter

of infrared energy ($\epsilon = .986 \pm 0.1$) in the infrared region beyond several microns in wavelength [22]. Since the emissivity of the skin is so near to unity, the amount of infrared radiation from an area is closely representative of the actual temperature of that area.

3.2 Imaging processing

When we attempted to follow the progression of burns during recuperation, we accomplished this by processing images that had been acquired on multiple occasions during the recovery process. The images were then processed by a Fortran program called BURN (see appendix) which consisted of seven steps:

1. Thresholding
2. Noise removal
3. Boundary retrieving

4. Area calculation
5. Finding major axis
6. Geometric transformation
7. Gray level interpolation

3.2.1 Thresholding

Thresholding is one of the most important approaches to image segmentation.

An image is described as a gray level distribution $p(x, y)$ composed of dark objects (e.g, burned skin on light skinned individuals) on a light background (normal skin on light skinned individuals), such that object and background pixels have gray levels grouped into two categories. Selecting a threshold T is an obvious way to separate the object pixels from the background pixels [23]. Then, any point (x, y) for which $p(x, y) \geq T$ is called a background point; otherwise, the point is called an object point. We then create a threshold

image $q(x, y)$ by defining,

$$q(x, y) = \begin{cases} 0 & \text{if } p(x, y) < T \\ 255 & \text{if } p(x, y) \geq T \end{cases}$$

Pixels labeled 0 correspond to objects (burned light skin) while pixels labeled 255 correspond to the background (normal light skin).

3.2.2 Noise removal

After thresholding, one still can not distinguish between object and noise in the image. In general, it is possible to remove most of the noise and rebuild the image so that the object is more clearly delineated. This can be accomplished by analysing the eight pixels which surround any individual pixel of interest. If more than four register as black points, the center pixel is considered as black (gray scale 0). If less than four register, than the pixel is registered as white (gray scale 255). If exactly four register as black, than

the original gray scale signal of the center pixel is kept.

3.2.3 Boundary retrieving

After removing the noise on the picture, the boundary of the burn area should appear as a cluster as shown in Fig 4.



Figure 4

An arbitrary pixel \otimes is selected inside this cluster, and the right most pixel horizontal to the previous pixel is then located (\odot) and designated as the initial pixel. To find the boundary of the cluster from the initial point, a

modification of the Chain code procedure was used [23]. In this procedure, the adjacent pixels to a center pixel are each assigned arbitrary numbers as shown in figure 5.

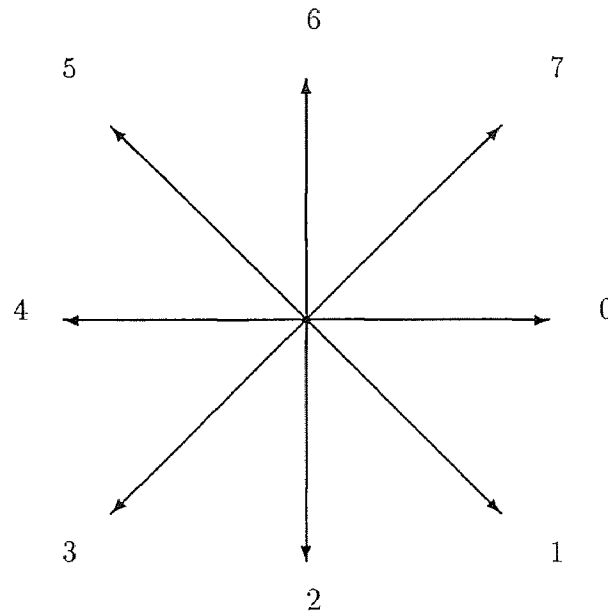


Figure 5

These numbers are assigned according to their direction from the center pixel. This "direction value" is used by the program to find the next pixel. For the initial pixel in figure 6, the direction value is first assigned as 0. In order to find the next pixel on the boundary, the program scans clockwise from

0 until the next pixel is encountered. When the next pixel is encountered, the program assigns the current direction value as that which corresponds to the direction which the initial pixel was in relation to the newly selected pixel. The computer then scans clockwise from the current direction value until the next pixel is encountered, and the process is thus repeated. Figure 6 shows the results when the whole boundary retrieval analysis is completed. The number beside each pixel corresponds to the direction value which was assigned when that pixel was encountered by the program.

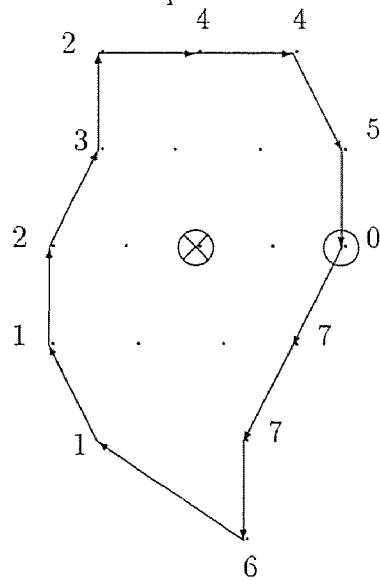


Figure 6

3.2.4 Area calculation

The area of a region can be described by the number of pixels contained within its boundary. We used polygon geometric analysis in order to determine this. Figure 7 shows the dimensions of the simplest possible polygon, a triangle, whose area can be described by the formula, $\frac{1}{2}[(y_1 + y_2)(x_1 - x_2) + (y_3 + y_1)(x_3 - x_1) + (y_2 + y_3)(x_2 - x_3)]$. Determination of the area of a polygon is performed by extending the equation appropriately to

$$\frac{1}{2} \sum^n (y_i + y_{i+1})(x_i - x_{i+1})$$

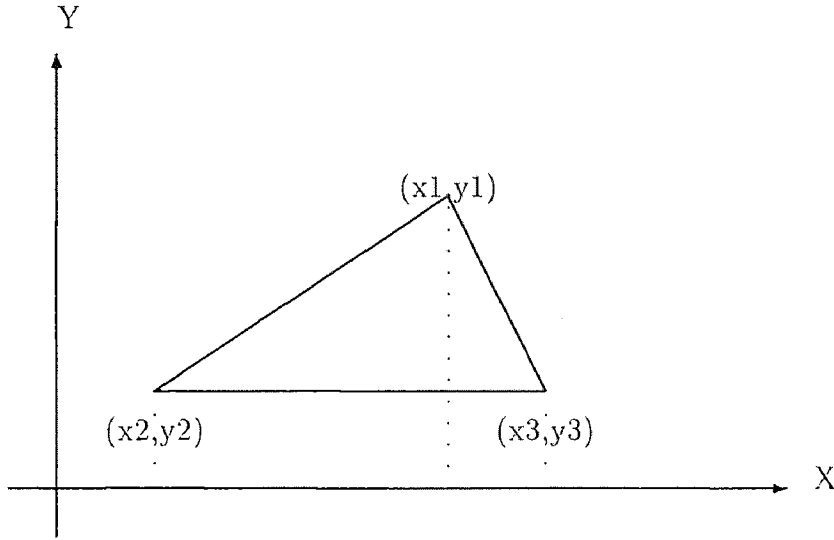


Figure 7

3.2.5 Finding major axis

When two pictures of a scene are taken at different times, the points at which they registered different can be determined, and thus the changes can be analyzed. The program compares the gray levels of all the pixels in the first image with those of the second image. In order to accomplish this, the program must first determine the major axis of each image, and then superimpose them by geometric transformation. The major axis is defined as the largest distance between two pixels on opposite sides of the boundary

(figure 8)[23]. By counting the number of pixels along the boundary, a rough approximation of its length can be obtained.

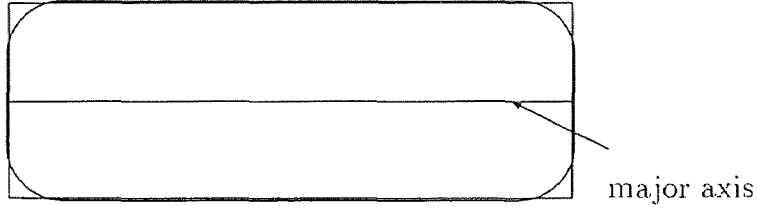


Figure 8

The diameter of a digital polygon boundary is defined as

$$Diam(B) = \max_{i,j} D(P_i, P_j)$$

where D is distance and P_i and P_j are points on the boundary.

3.2.6 Geometric Transformation

- The rotation angle of the major axes of the first original (base) and second (input) images are computed from the coordinates of the major

axis limits as shown below for the base image only.

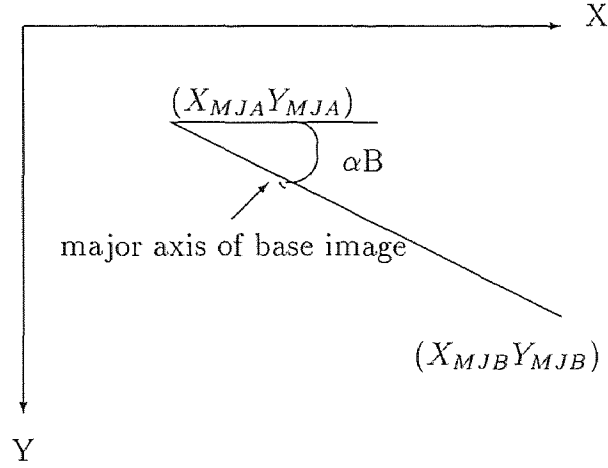


Figure 9

where,

$$\alpha_B = \tan\left(\frac{Y_{MJB} - Y_{MJA}}{X_{MJB} - X_{MJA}}\right)$$

the difference between angles of the two image's axes is therefore the rotation angle.

- Spatial transformation:

An object displayed by the image processing system is made up of numerous points, each with specific (x,y) values in a two dimensional

planar coordinate system. If the object Obj is moved to a new position, it can be regarded as a new object Obj', all of whose coordinate points (P) can be obtained from the original points (P') by the application of a geometric transformation [24].

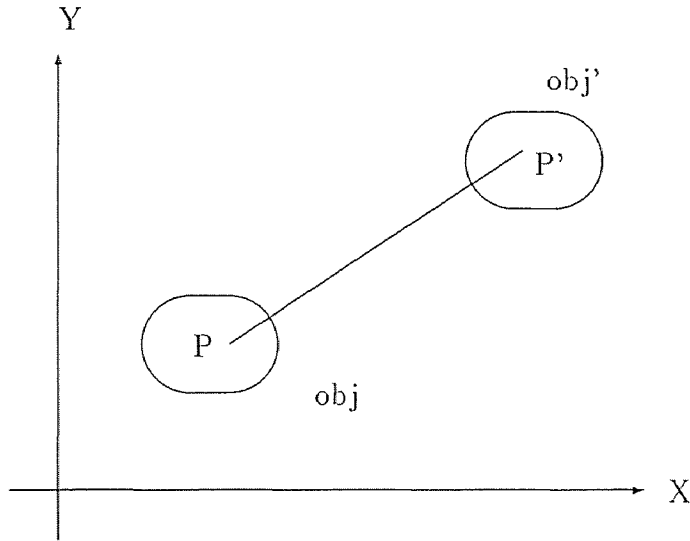


Figure 10

(a) Translation:

In translation, an object is displaced a given distance and direction from its original position. If the displacement is given by the vector $v = t_x I + t_y J$, and we wish to translate a point with coordinates (x, y) to a new

location by using displacements (h,k), the translation is accomplished by using the following equations:

$$x' = x + t_x$$

$$y' = y + t_y$$

where (x', y') are the coordinates of the new point. The equation may be expressed in matrix form by writing

$$\begin{bmatrix} x' \\ y' \end{bmatrix} = \begin{bmatrix} 1 & 0 & t_x \\ 0 & 1 & t_y \end{bmatrix} \begin{bmatrix} x \\ y \\ 1 \end{bmatrix}$$

The notational representation of this process is simplified considerably by using square matrices, and we may then write the equation in the following form:

$$\begin{bmatrix} x' \\ y' \\ 1 \end{bmatrix} = \begin{bmatrix} 1 & 0 & t_x \\ 0 & 1 & t_y \\ 0 & 0 & 1 \end{bmatrix} \begin{bmatrix} x \\ y \\ 1 \end{bmatrix}$$

We then use the unified matrix representation $V^* = TV$. Using this notation, the matrix used for translation is given as

$$T = \begin{bmatrix} 1 & 0 & t_x \\ 0 & 1 & t_y \\ 0 & 0 & 1 \end{bmatrix}$$

$$V^* = \begin{bmatrix} x' \\ y' \\ 1 \end{bmatrix} ; V = \begin{bmatrix} x \\ y \\ 1 \end{bmatrix}$$

(b)Rotation:

The displacement of a point from position (x,y) to position (x', y') , as determined by a specified rotation angle θ relative to the coordinate origin angle

ϕ , is the original angular position of the point from the horizontal [25]

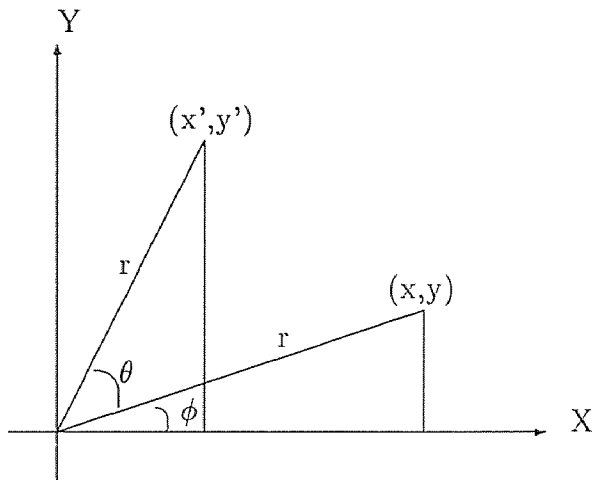


Figure 11

Using triangles and standard trigonometric identities, we can write

$$x' = r \cos(\phi + \theta) = r \cos \phi \cos \theta - r \sin \phi \sin \theta$$

$$y' = r \sin(\phi + \theta) = r \sin \phi \cos \theta + r \cos \phi \sin \theta$$

where r is the distance of the point from the origin. Also,

$$x = r \cos \theta, y = r \sin \theta$$

so that the equation can be restated in terms of x and y as

$$x' = x \cos \phi - y \sin \phi$$

$$y' = y \cos \phi - x \sin \phi$$

Objects can be rotated around an arbitrary point by a modified equation adapted to include the coordinates (h, k) for the selected rotation point. The transformation equations for the rotated coordinates can be obtained from the trigonometric relationships depicted in figure 12, and can be written as

$$x' = h + (x - h) \cos \theta - (y - k) \sin \theta$$

$$y' = k + (y - k) \cos \theta + (x - h) \sin \theta$$

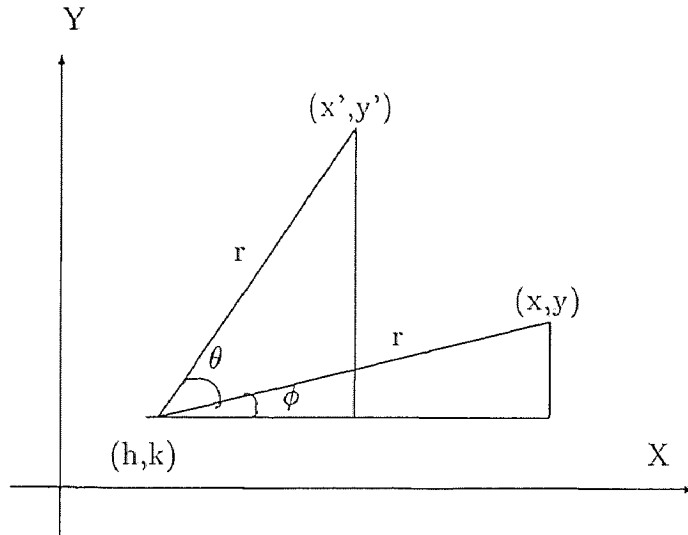


Figure 12

so we get the matrix

$$R = \begin{bmatrix} \cos \theta & -\cos \theta & (-h \cos \theta + k \sin \theta + h) \\ \sin \theta & \cos \theta & (-h \sin \theta - k \cos \theta + k) \\ 0 & 0 & 1 \end{bmatrix}$$

(c) Total transformation matrix

If rotation angle is r , then the transformation matrix can be described as the

product of the rotation matrix R and the translation matrix T :

$$Q = R \times T$$

so we therefore get

$$x_1 = x \times \cos(r) - y \times \sin(r) + [(t_x - h) \times \cos(r) - (t_y - k) \times \sin(r)] + h$$

$$y_1 = x \times \sin(r) + y \times \cos(r) + [(t_x - h) \times \sin(r) + (t_y - k) \times \cos(r)] + k$$

(d) Matrix size

If all the conditions in the above can be satisfied, we can then create boundary boxes for both base and input images. However, in order to ensure that operations do not result in any part of the image falling out of bounds, we have to consider the following figure.

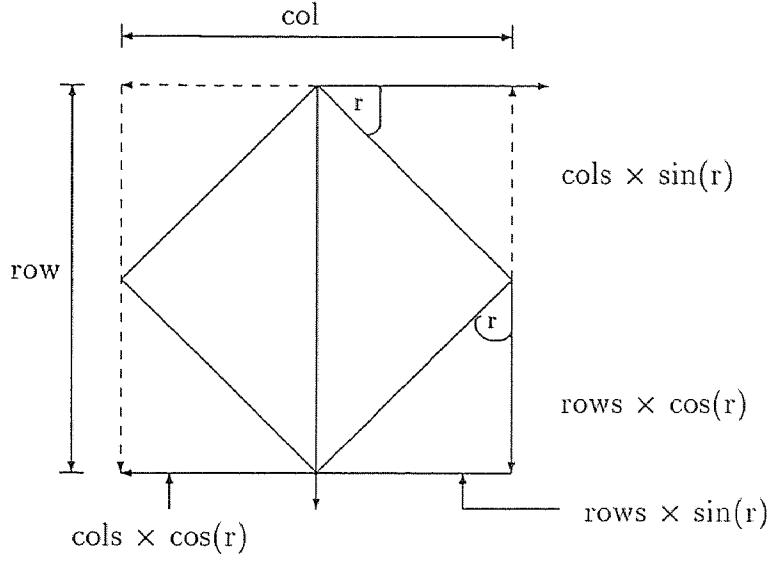


Figure 13

For this diagram, we have

$$row = cols \times \sin(r) + rows \times \cos(r)$$

$$col = cols \times \cos(r) + rows \times \sin(r)$$

where col and row are the width and height of transformed matrix Q . In summary, no matter in which quadrant the angle lies, the predicted size of matrix will be

$$col = cols \times |\cos(r)| + rows \times |\sin(r)|$$

$$row = cols \times |\sin(r)| + rows \times |\cos(r)|$$

The program ensures that conditions are met to prevent any part of the image going out of bounds.

3.2.7 Gray level interpolation

The above method proceeds through integer values of the coordinates (x,y) until the corrected image p(x,y) is produced. However, the above equations can yield non-integer values for x' and y' , thus causing a mapping into locations of p (x,y) for which no gray levels are defined [26][27][28].

To convert the results of the transformation into a digitized picture, the new values must be interpolated to coordinates for which gray levels are assigned. This is accomplished by bilinear interpolation. The procedure is illustrated as follows: let the integer parts $[x'']$, $[y'']$, of x'' and y'' be i and j respectively, so that the point (x'', y'') is surrounded by the four-integer-coordinate points (i, j+1), (i+1, j), (i, j), (i+1, j+1). Let the fractional parts

of x'' and y'' be ,

$$\alpha = x'' - [x''] \quad and \quad \beta = y'' - [y'']$$

thus

$$0 \leq \alpha, \beta \leq 1$$

then the gray level that we assign to (x', y') is given by

$$f(x', y') = (1 - \alpha)(1 - \beta)f(i, j) + (1 - \alpha)\beta f(i, j + 1)$$

$$+ \alpha(1 - \beta)f(i + 1, j) + \alpha\beta f(i + 1, j + 1)$$

4 RESULT AND DISCUSSION

Results from the model surface area were compared with estimates computed using the computer program BURN. BURN program calculations were easily performed, and did not significantly vary with changes in user. A percent error analysis revealed an acceptable range from 0.07% to 2.8% for the rectangular aluminum plates that were used to simulate burns on the hand. The experimental results are summarized in Table 4. From this calibration data it is clear that the BURN program can make reasonably accurate estimates of the simulated burn area, and could therefore be used to produce acceptable estimates of real skin burn area.

	1	2	3	4	5	6
Real Area Value(cm^2)	20	9	8	6	21	10
Measured Value(cm^2)	20.5648	9.1905	7.994	5.9003	20.466	9.978
Error(%)	2.8	2.1	0.07	1.66	2.54	0.22
Average Error = 1.565% 1 pixel = $9.94 \times 10^{-4} cm^2$						

Table 4 Six sizes of simulated surfaces were used in these studies

If we had a hospitalized patient with partial thickness burns of the torso, the total burn area could be assigned to several different regions. Regimen A is defined as the wound area which was treated by medicine A. Regimen B is defined as the wound area which was treated by medicine B. At each time point we could take imaging data from both the regimen A and B areas. The burn areas being treated by each regimen will decrease but the degree of recovery will depend on the treatment modality. The BURN program should be able to help us calculate recovery rates by measuring the time dependent area changes in the different areas of burned skin. This is illustrated using the model system.

Figure A1 illustrates an image of an aluminum plate on a volunteer's hand. Figure A2 represents a boundary analysis of the image in figure A1. By superimposing the two images it can be shown that the boundary retrieval analysis does indeed depict limits of the aluminum plate as depicted in figure A1. Figure A3 illustrates an image of a smaller plate which was worn in a

different position in front of the camera. Using an auto rotation facility in the BURN program, the boundary retrieval analysis of this image could be rotated as shown in figure A4. This proved a useful technique for comparing the sizes of different images, as shown in figure A5, which depicts the result of superimposition of the boundary image of figure A4 on the original image in figure A1. Hence for burn analysis this allowed us to consider using the system to compare burn sizes at different times without the need to maintain a specific angle of imaging for both pictures, thus limiting any inconvenience which might otherwise be imposed on patients.

It has been known for some time that there is a relationship between burn temperature and depth. Before we discuss the burn depth, let us consider the measurement of skin temperature. For a specific spectral interval $\Delta\lambda$, we know that the total energy radiated throughout the spectrum per second by a surface 1cm^2 in area, in watts per cm^2 , is given by $W = \epsilon\sigma T^4$. We could

then write

$$W_{\Delta\lambda} = K\varepsilon_{\Delta\lambda}T^n$$

where the exponent n varies with λ and represents the effective average value throughout $\Delta\lambda$, and $W_{\Delta\lambda}$ is expressed as watts per cm^2 per $\Delta\lambda$ [13]. In our studies we wish to compute temperatures and/or temperature differences, ΔT . It is clear that we can obtain images of the same intensities from two objects of different temperatures, provided their respective $\varepsilon_{\Delta\lambda}$'s vary by the correct amount. If we were to ignore the variation of the $\varepsilon_{\Delta\lambda}$'s, we would introduce an error in the estimation of temperature. Therefore, it is necessary to know $\varepsilon_{\Delta\lambda}$ in order to compute T . Unfortunately, it is usually very difficult to measure $\varepsilon_{\Delta\lambda}$ exactly and as such, there are limits to the accuracy of all such temperature determinations.

In general, it is easier to calculate the percentage change in the temperature of a given object, or the ratio of two temperatures, than it is to determine an absolute temperature. If we measure $W_{\Delta\lambda}$ for a single object

at two different times, we can immediately determine the ratio of the two T 's, even though $\varepsilon_{\Delta\lambda}$ may be unknown. As described in the above discussion, we know how to measure the percentage change in temperature for two areas of human skin whose temperature's are directly proportional to their respective $W_{\Delta\lambda}$'s. In this thesis, we are primarily interested in comparing the temperatures between normal skin areas and a burn area. Fortunately, most skin temperatures fall somewhere between 300 K and 310 K, which is within ± 1.6 percent of a mean value of 305 K. The measured ratios would then be estimated with an accuracy no worse than ± 1.6 per cent using 305 K as the reference. Since the extreme range of skin temperature is rarely encountered, the computed ΔT 's are normally even more precise, and the residual error is negligible.

The human body emits infrared waves between 2 and 20 μ in wavelength, and in the wavelengths beyond 3 μ , the emissivities of human skin are very close to unity within one or two per cent [22][29]. We can then assume that

for each different temperature the intensity variations of a theoretical black body shown on infrared imaging would correspond to true skin temperature variations. Fig B shows the gray scale that would be obtained from a theoretical black body. We can use this gray scale to calibrate the temperature of the skin area. We found that on average, each gray scale increment is 0.1°C in the range between 30 to 40°C .

We processed infrared images from a female patient (plate 1) who was admitted with third degree right breast burns (figure C1) and second degree left breast burns (figure D1), When images were analyzed, we found that the third-degree burn areas were colder than normal skin and appeared as dark gray or black. Areas of second-degree burns were colder than normal skin, but not as cold as the third-degree burn areas [30]. Figure C2 shows the result of image analysis from the right breast third degree burn taken one day later than the analysis depicted in figure C1. When comparing the data in figure C1 and figure C2 , we see that the burn area had decreased detectably

over time. Boundary retrieval analysis also confirmed these findings (figure C3 and C4 respectively). In addition, the burn area imaged in figure C2 had a higher temperature as compared to that imaged in figure C1. A graph of the gray level distribution from the burnt areas in figure C1 and figure C2 is illustrated in figure C7. The x-axis on figure C7 refers to individual gray level values, and the y-axis refers to the total number of pixels in the original figures that possessed those individual gray level values. From the figure we can compute by interpolation the average gray level value from each of the distributions as 88.97 for figure C1 and 129.3 for figure C2. The average value is that at which the total number of pixels with higher gray level values is equivalent to the total number with values below.

Unfortunately, the burn area images as depicted in figure C1, C2 and D1 did not allow us to easily visualize exact changes in temperature in different areas of the picture. Also, the graph analysis of the gray areas fails to provide positional information on exact changes in temperature distribution.

In order to circumvent these problems, we used a color graphics feature (color thermography) to display the images. Color thermography is useful since it can display temperature differences polychromatically, which allows us to determine temperatures more easily (within a range) by eye [31]. In our case we used it to display 16 different levels in the 0 to 255 gray scale range (figure C8). This corresponded to 16 gray scale increments per color, or in other words a $\Delta 1.6^{\circ}\text{C}$ in each color. The system could potentially be set to optically determine narrower changes in temperature down to 0.1°C if the temperature range was suitably delimited, however, this was beyond the capabilities of the BURN program we were using. In any case, using color thermography greatly improved our visualization of the burn areas.

It is well established that the time that burns take to heal is largely dependent on their depth [30]. Full thickness (third degree) burn areas remain as “cold spots” until such time as they are treated by grafting. In our own studies on the woman patient, color thermographic analysis of figures C1 and

C2 (figures C5 and C6 respectively) revealed that burn temperature, as well as size, changed over time. The average temperature over the burn area in figure C5 was determined to be $2\frac{1}{2}^{\circ}C$ below that of normal skin. The peak decrease in temperature at the center of the burn was $11^{\circ}C$ below normal. Figure C6, which shows analysis one day after recovery shows that peak temperature reductions at the burn center were around $8^{\circ}C$ below normal.

Figures E1 and E2 represent monochromatic and color thermographic image analysis (respectively) of first degree burns on a male burn patient (plate 2). These burns were diagnosed as first degree since they took less than one week to recover. Figure E2 clearly shows that the burn area was warmer than the surrounding normal tissue, thus confirming the first degree diagnosis. This was most likely due to the increased inflammation in the superficially damaged tissue which would give rise to erythema [31].

Increased microcirculation often results in various epithelial tissues which

are damaged only superficially [32]. Deeper vascular damage will interrupt the circulatory process and result in more widespread necrosis, and in a fall in skin surface temperature would be expected. When we analysed the female patient with second degree burns on her left breast by color thermography (figure D2), we found that burn temperature was between $2\frac{1}{2}$ and $1\frac{1}{2}^{\circ}\text{C}$ below that of normal skin. This burn took longer than one week to heal, which helped us diagnose the burn. With this burn, the damage probably did involve vascular tissue which would have resulted in decreased metabolism and circulation to the injured skin. Another observation taken from the woman patient concerned the temperature of tissue which had undergone granulation after burning (figure F1). This tissue was also colder than normal skin.

5 CONCLUSIONS

While the body maintains a fairly constant internal, or "core", temperature, skin temperature varies considerably with environmental temperature changes [30]. The main source of heat to the skin is that conducted to it from internal heat sources. Of course, factors other than environment and internal heat also affect skin temperature, such as metabolism, vascularity, and sweating. Pathological conditions that cause inflammation will show an increase in temperature which will arise as a result of increased microcirculation to the inflamed area.

Burn area, temperature and depth are three important factors which could be used to contribute toward the specific diagnosis of burns. Currently, diagnosis still depends heavily on semi-quantitative clinical examination and retrospective burn history. Early specific diagnosis will help decide the correct course of therapy more appropriately. Color thermography is an advanced method for determining these factors which may prove more useful

than simple clinical examination. It can distinguish first and second degree burns on the basis of the direction of temperature change, and second and third degree burns by the degree to which the temperature is reduced relative to normal skin. It would therefore appear to be a very useful tool in burn therapy.

Plate 1

Photograph of female patient studied with third degree right breast and second degree left breast burns.



Plate 2

Photograph of male patient with abdominal first degree burns.



Figure A1

Image analysis of a simulated burn area (aluminum plate) on human skin.

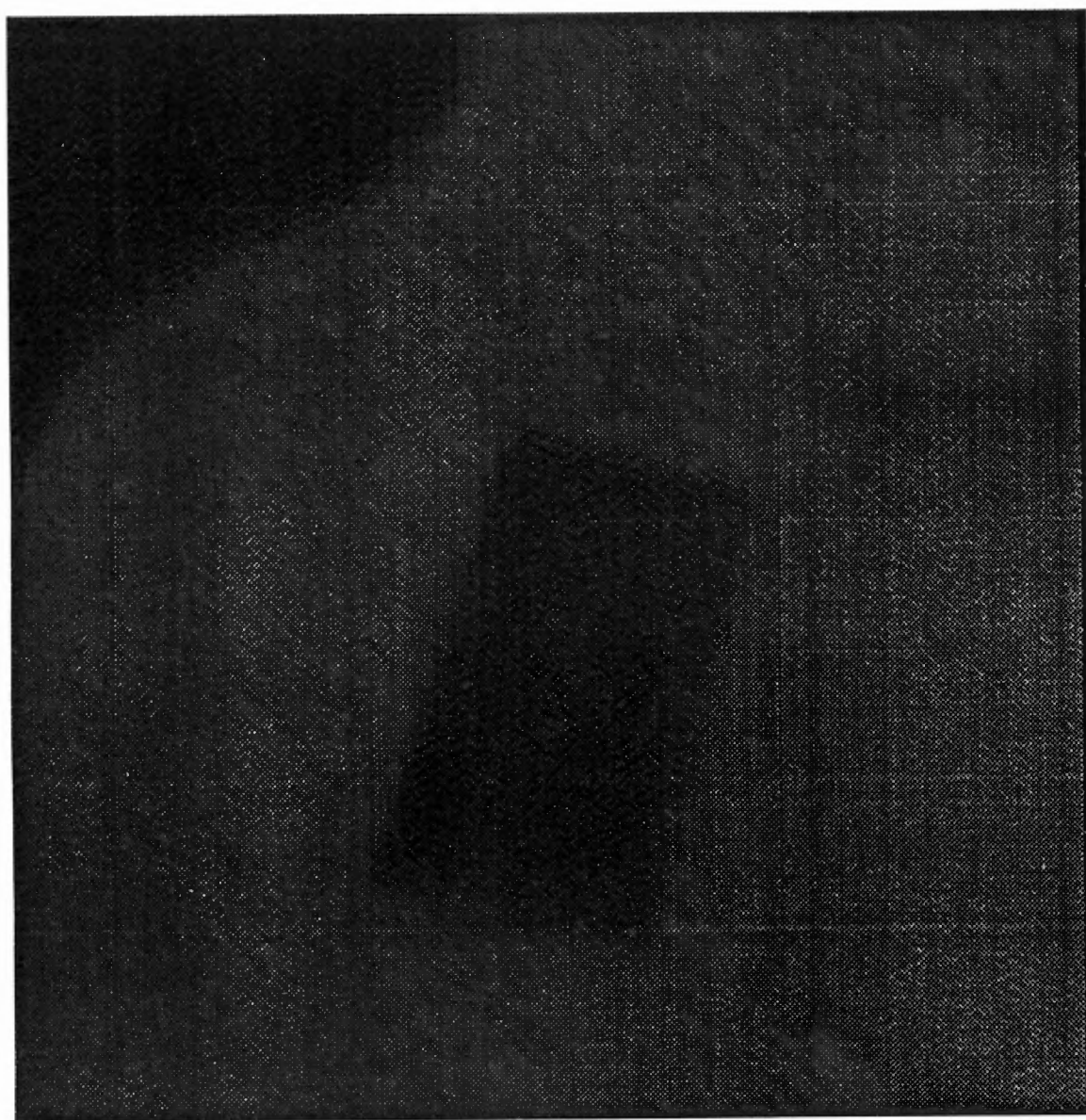


Figure A2

Boundary retrieval analysis of simulated burn area depicted in figure A1.

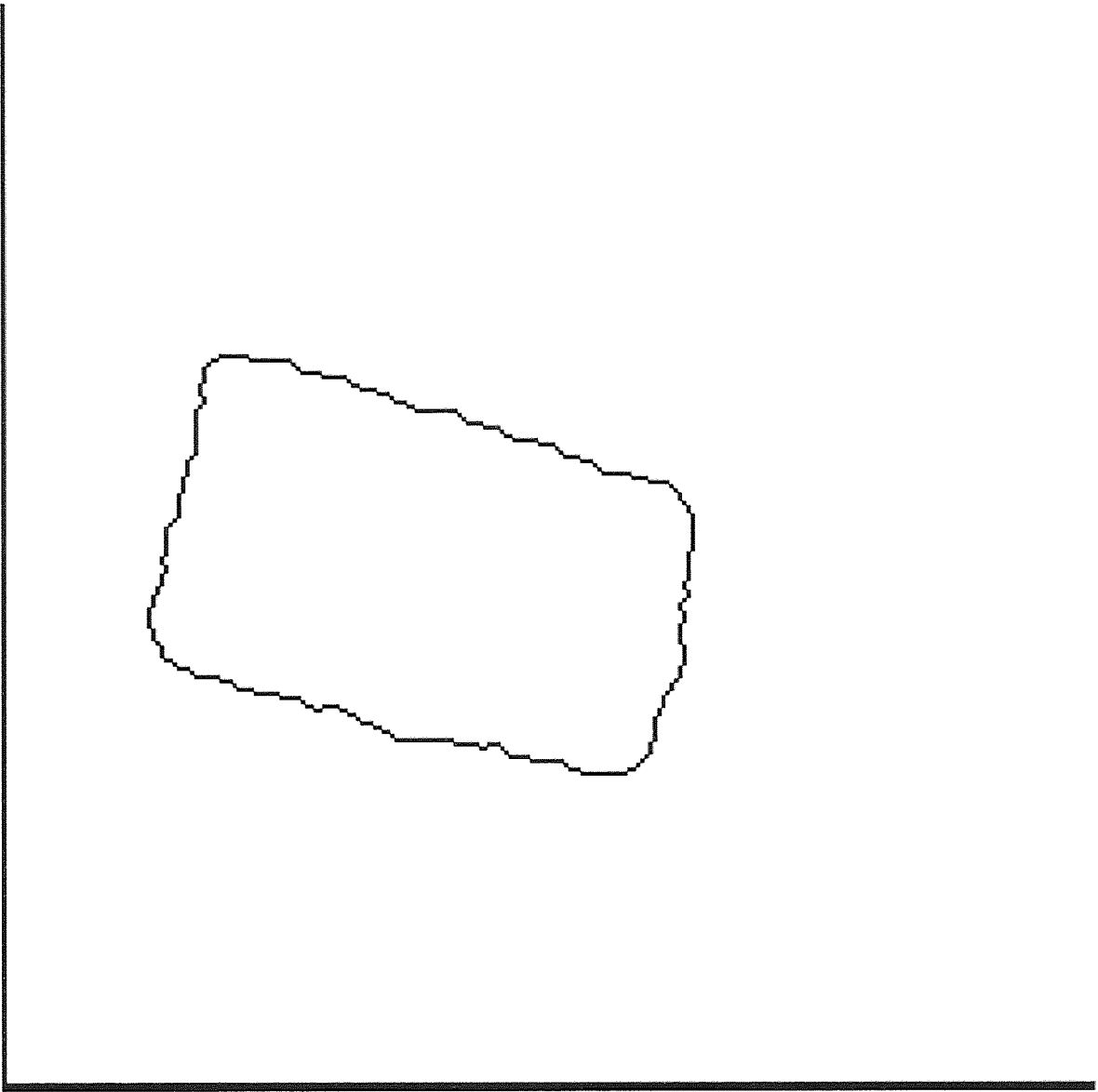


Figure A3

Image analysis of a small simulated burn area (aluminum plate) on human skin.

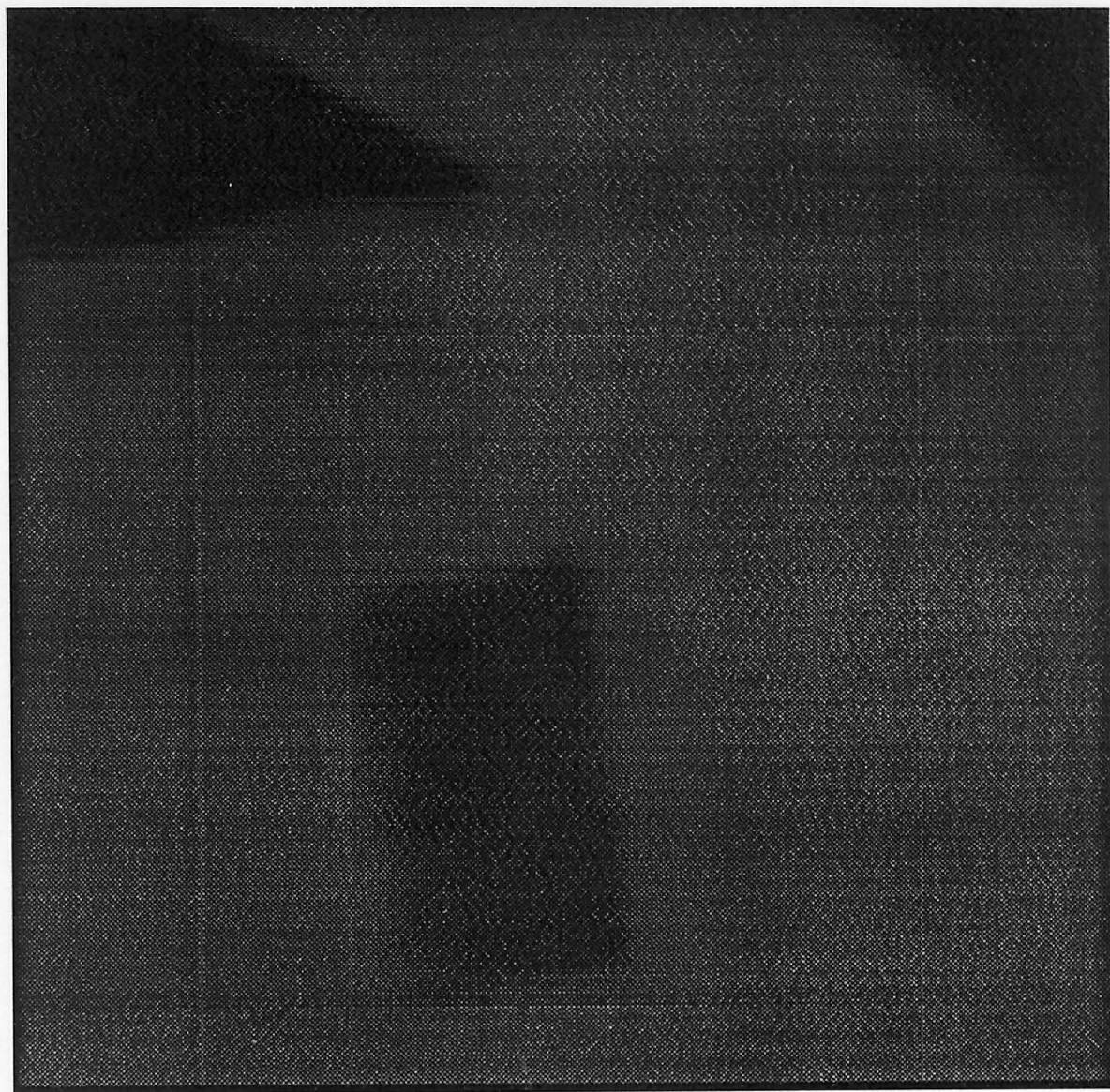


Figure A4

Boundary retrieval analysis of simulated burn area depicted in figure A3
after translocation and rotation.

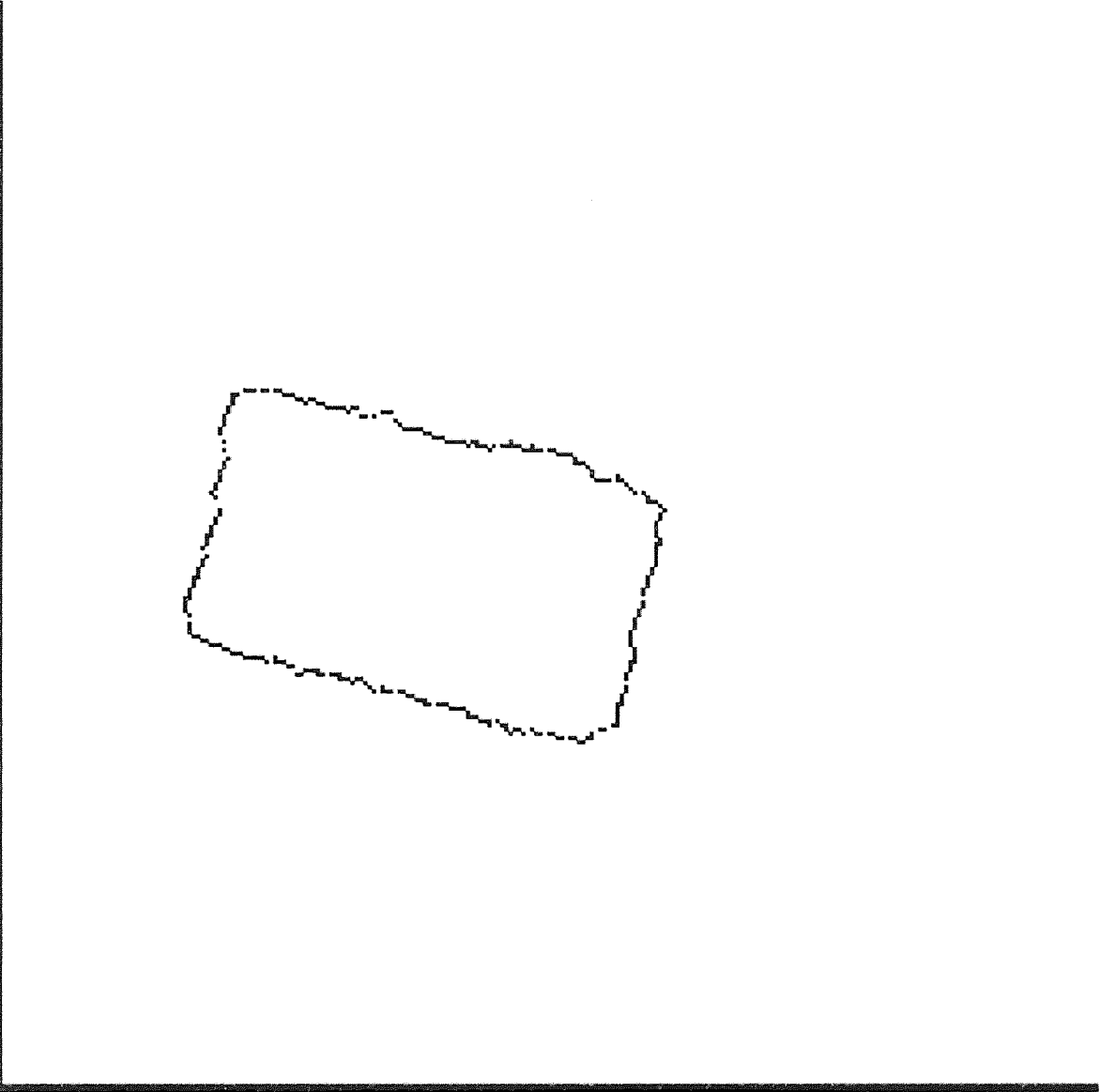
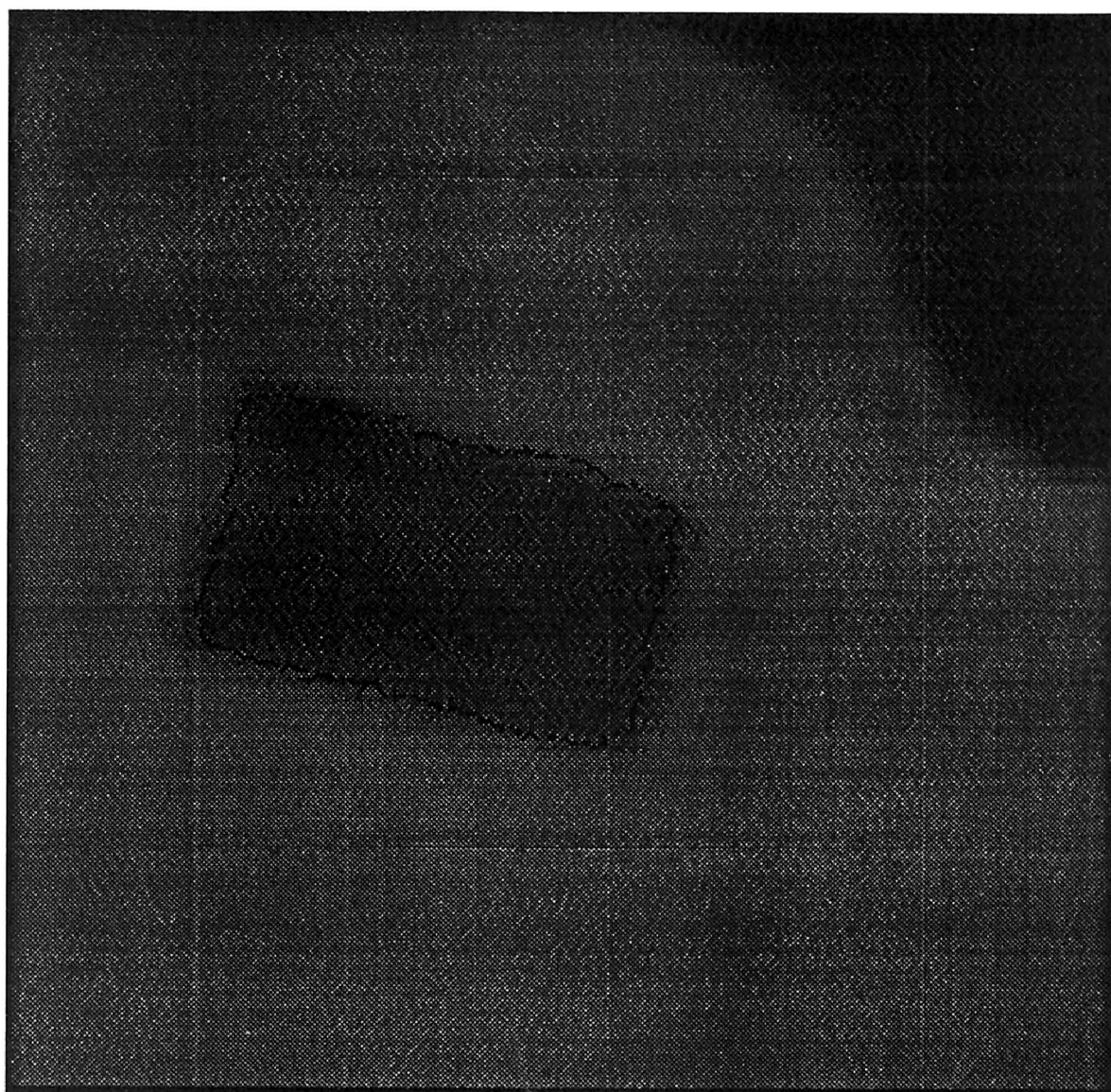


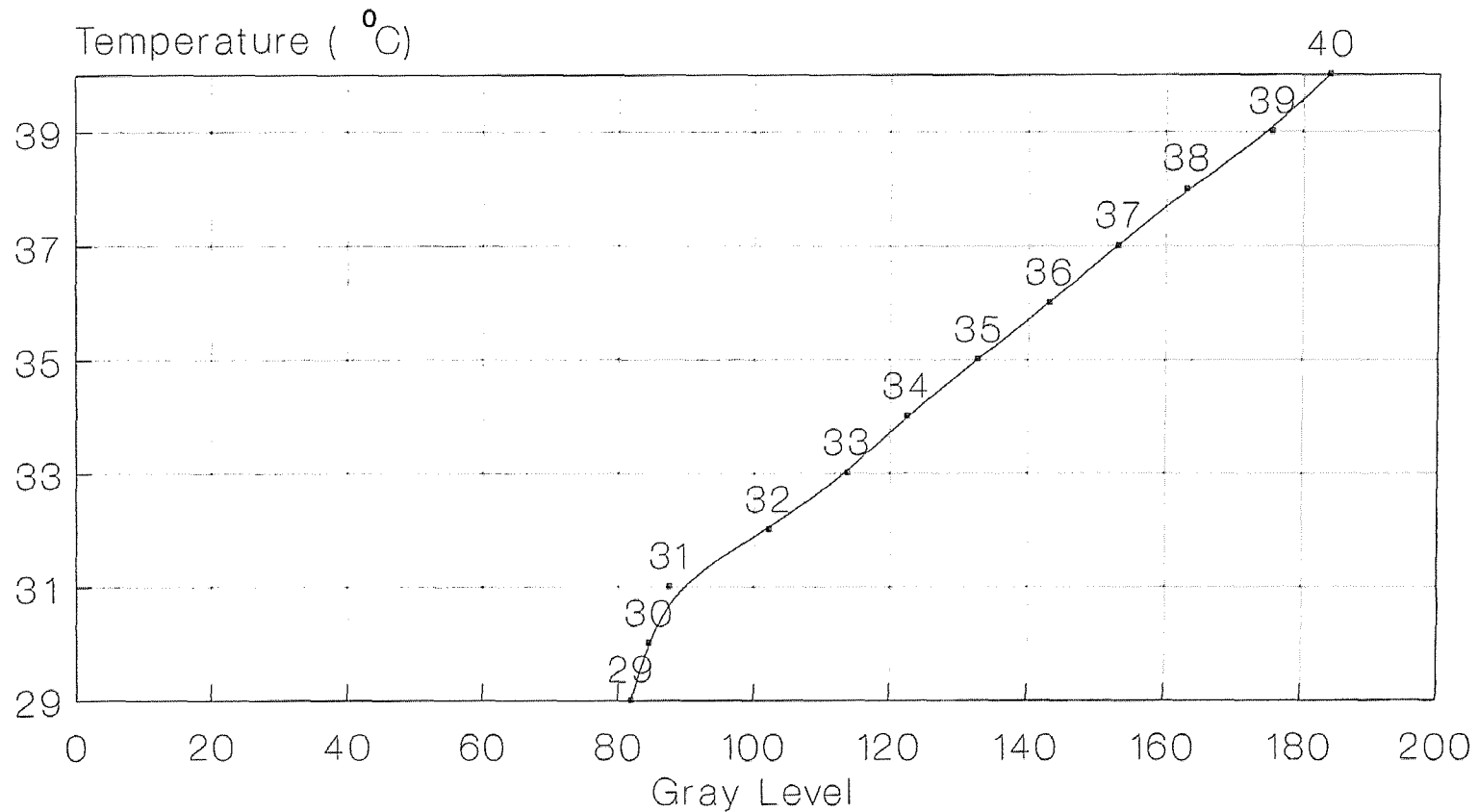
Figure A5

Superimposition of boundary analysis (figure A4) on image depicted in figure A1.



TEMPERATURE vs. GRAY LEVEL

Fig. B



—•— Gray Level

Gray scale obtained from a theoretical black body.

Figure C1

Image analysis of third degree right breast burn from a female patient
after hospital admission.

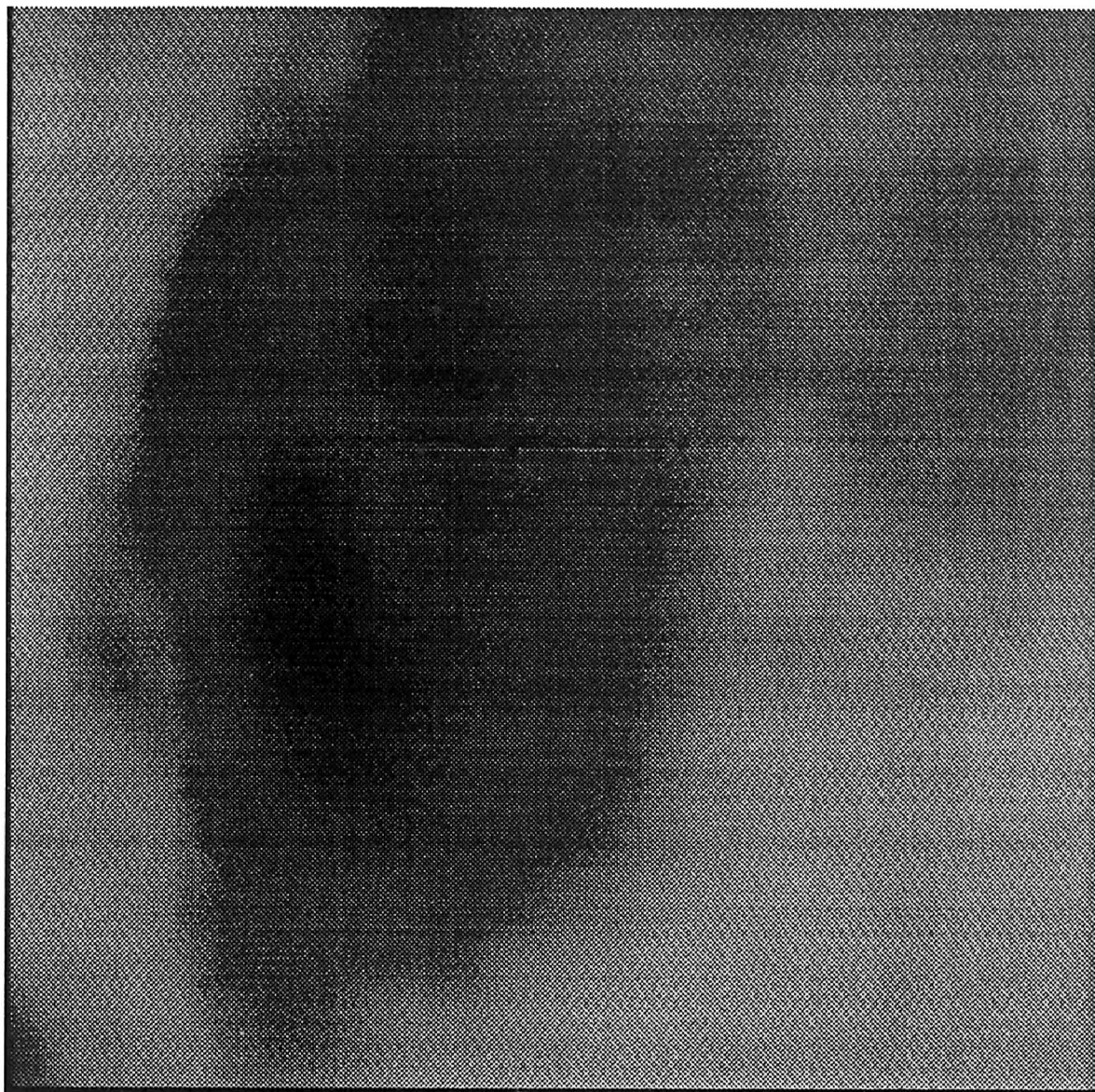


Figure C2

Image analysis of third degree right breast burn from figure C1 one day after figure C1 was recorded.

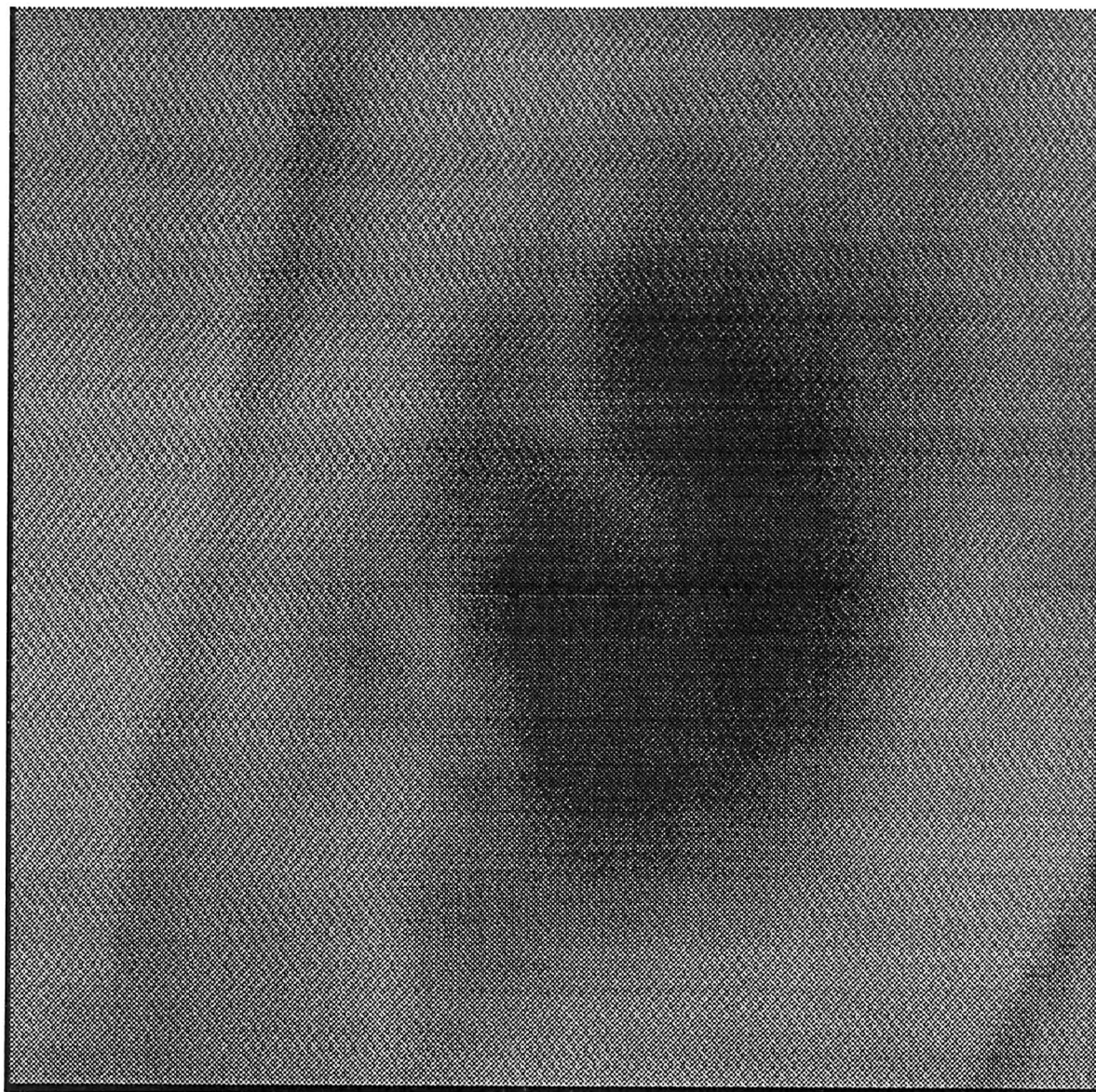


Figure C3

Boundary retrieval analysis of third degree right breast burn depicted in figure C1.

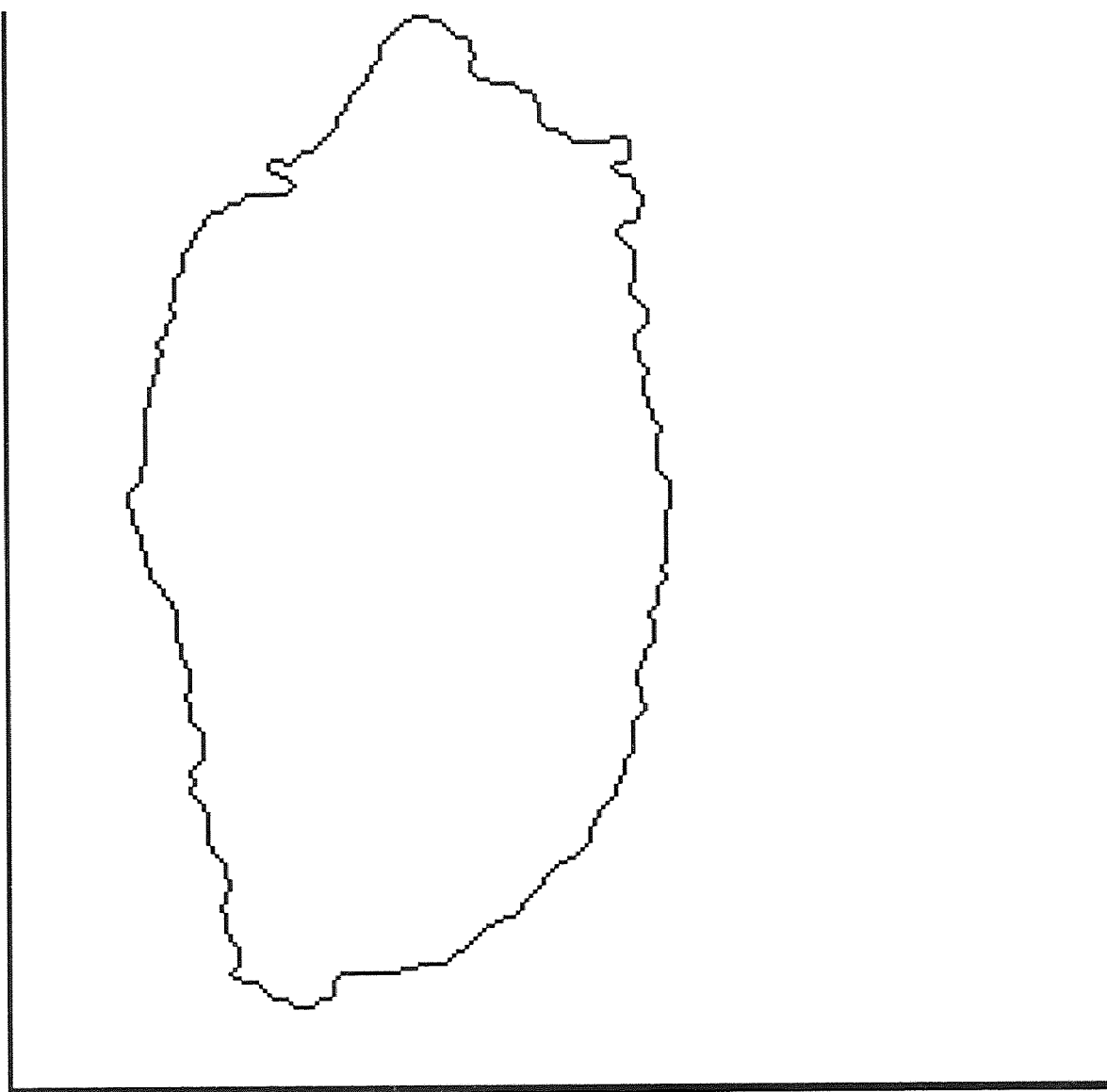


Figure C4

Boundary retrieval analysis of third degree right breast burn depicted in figure C2.

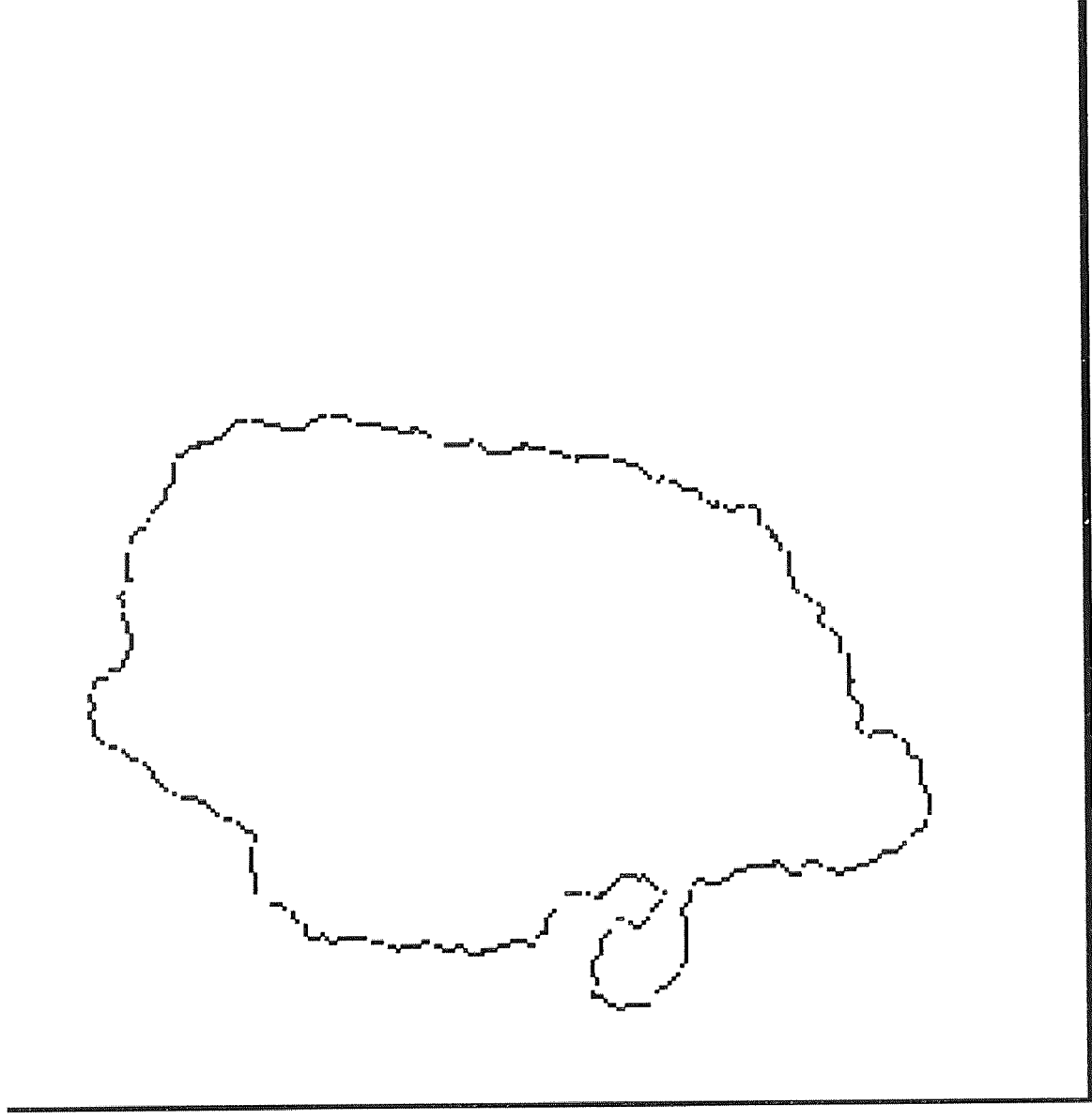


Figure C5.

Color thermographic analysis of third degree burn depicted in figure C1.

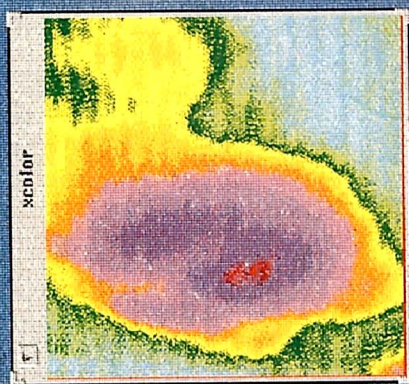


Figure C6.

Color thermographic analysis of third degree burn depicted in figure C2.

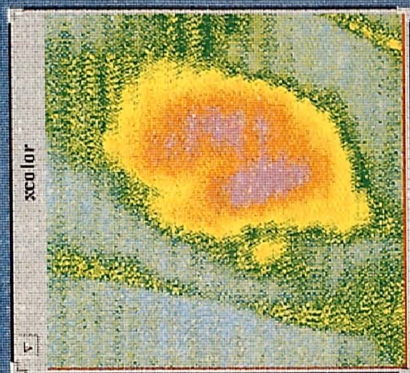
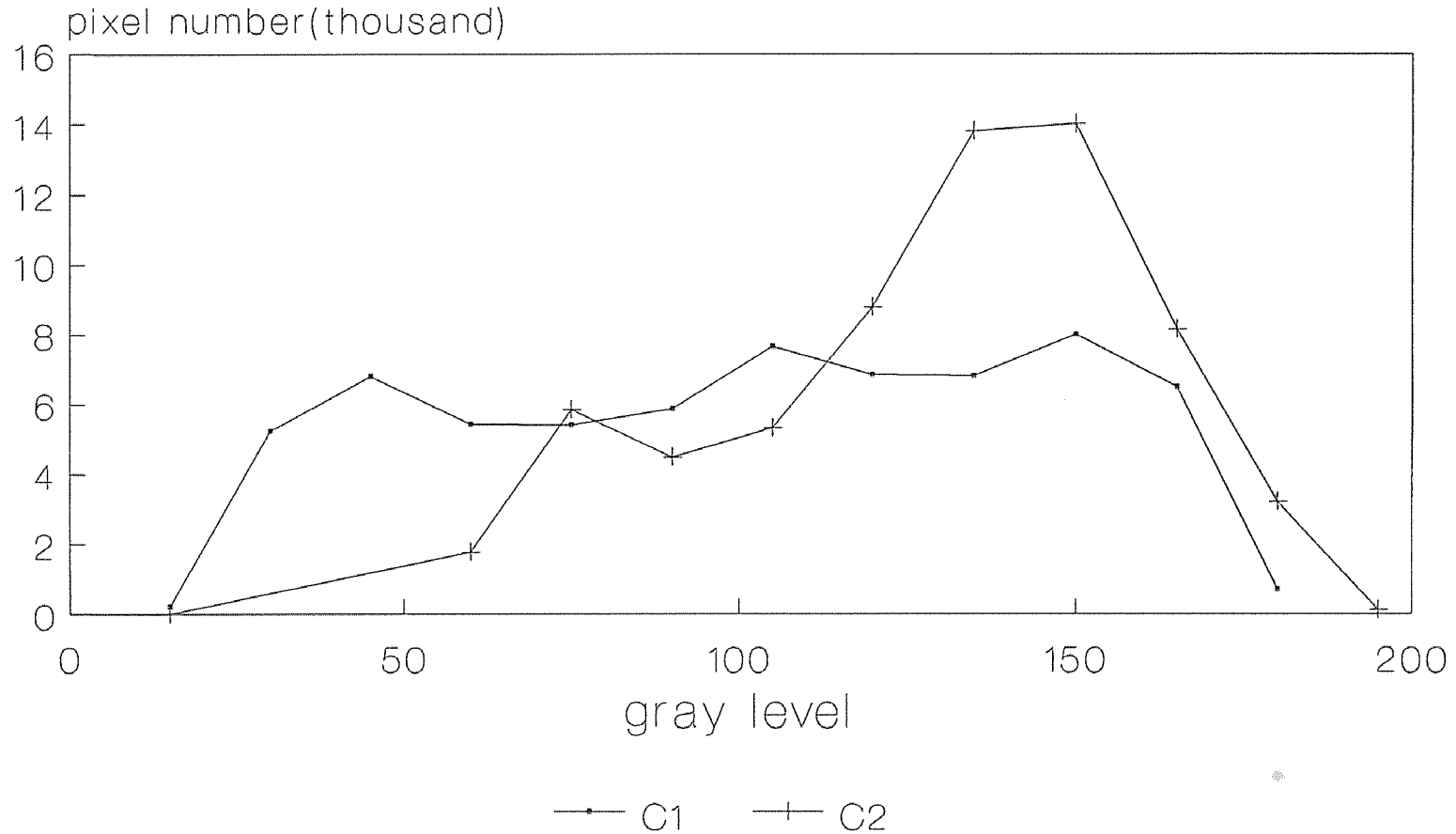


Figure C7.

Gray level distributions from image analysis depicted in figures C1 and C2. The y-axis describes the number of pixels on the picture which possess the gray level values depicted on the x-axis.

GRAY LEVEL HISTOGRAM

Fig C7



0(black,cool)<gray level<255(white,warm)

Figure C8.

Calibration diagram for color thermographic analysis. Each bar represents an increment of 1.6°C .

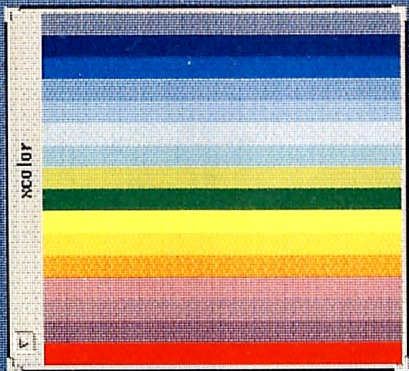


Figure D1

Image analysis of second degree left breast burn from female patient.

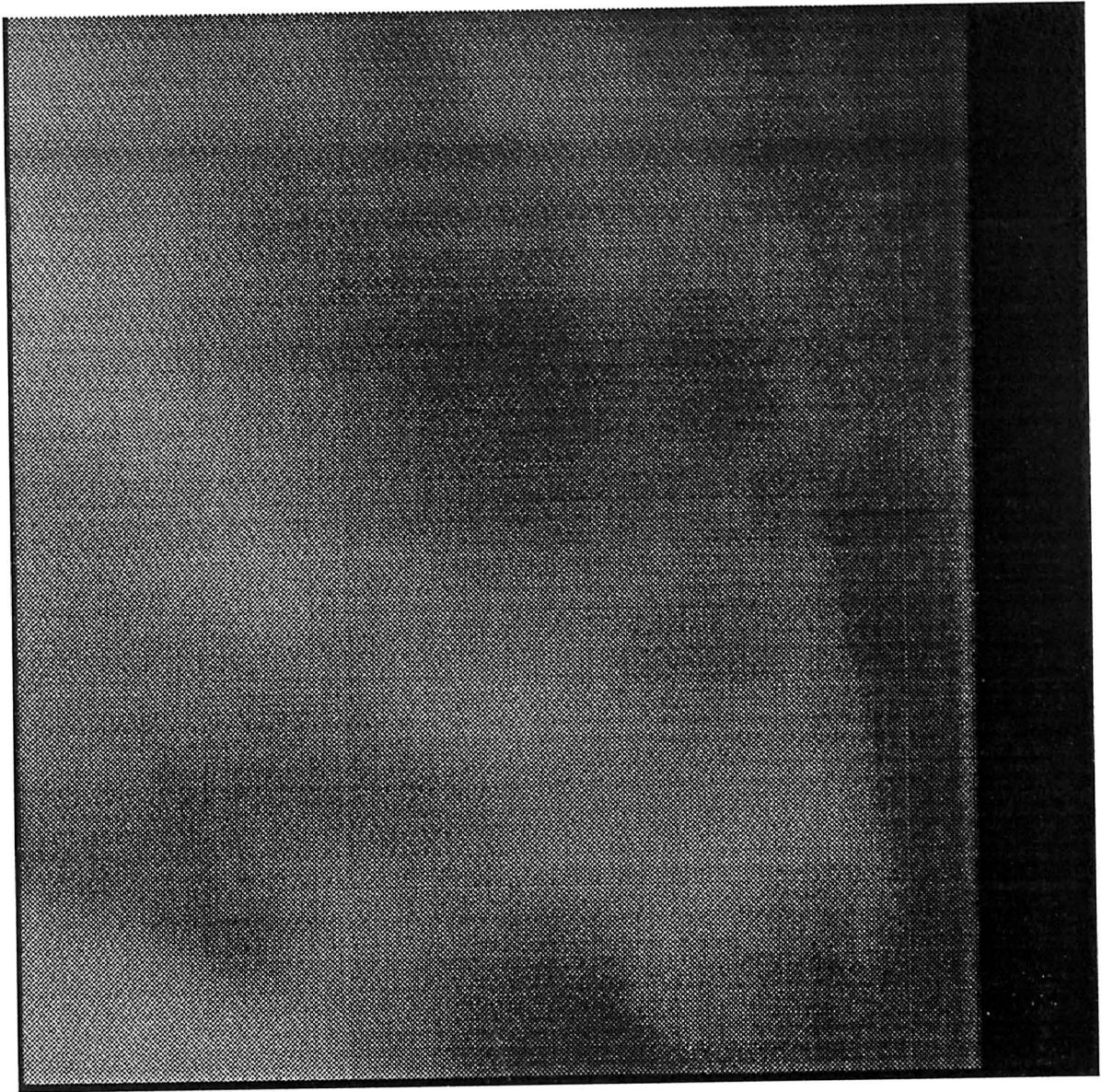


Figure D2

Color thermographic analysis of second degree right breast burn from female patient.

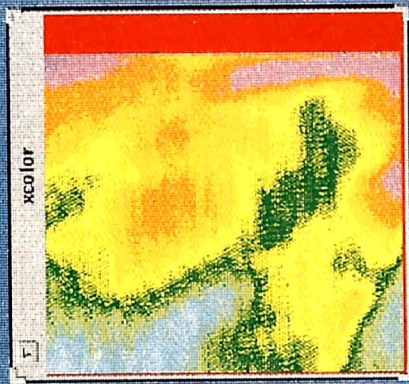


Figure E1.

Image analysis of first degree burn on the abdomen of a male patient.

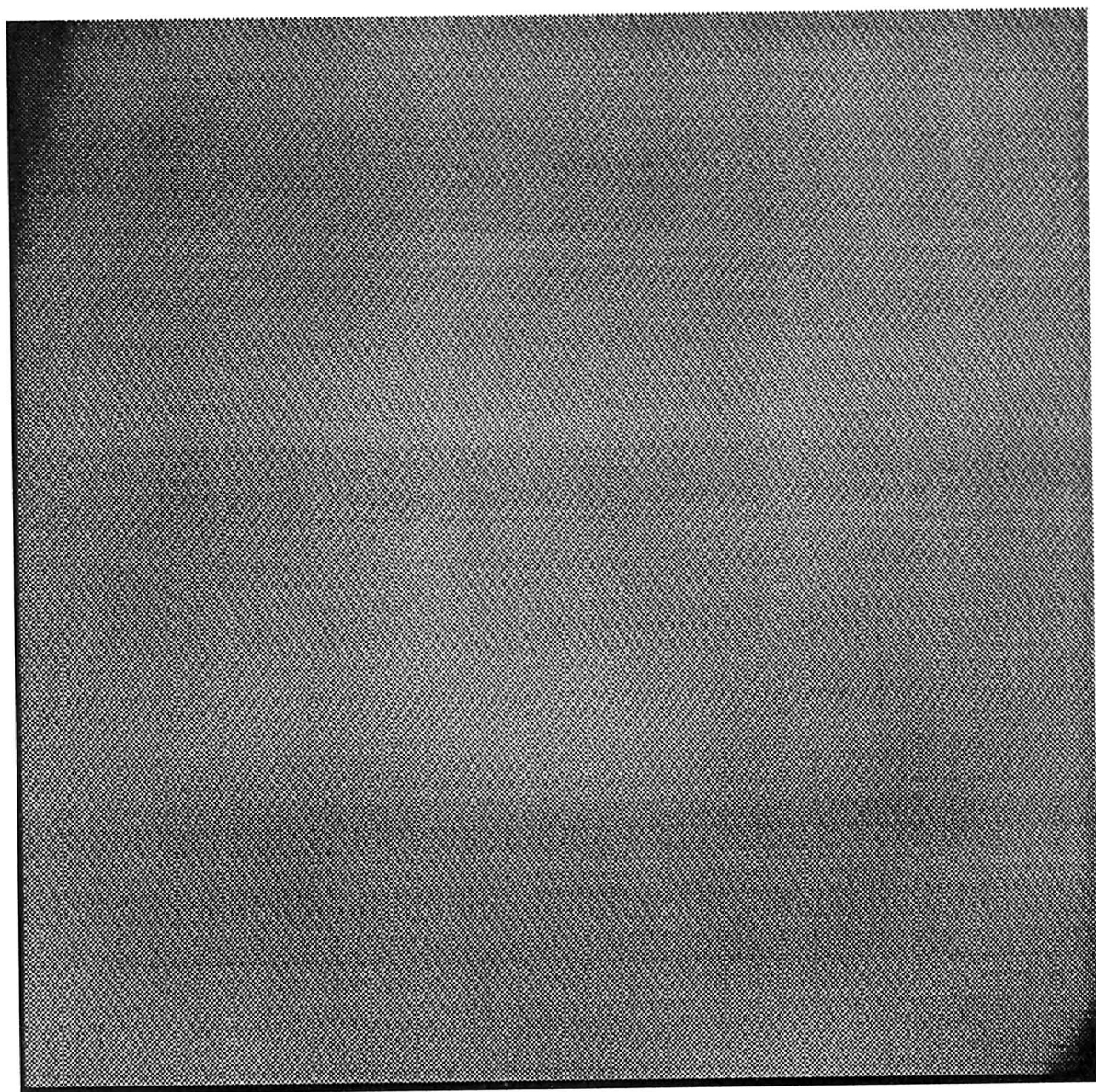


Figure E2

Color thermographic analysis of first degree burn depicted in figure E1.

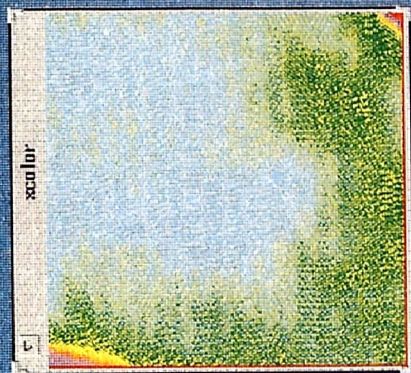
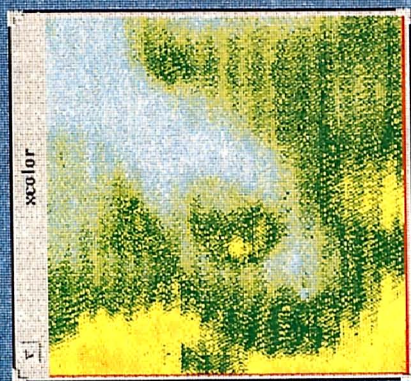


Figure F1

Color thermographic analysis of a region of burnt skin which had undergone granulation on the female patient.



6 REFERENCES

References

- [1] Holmes, T.: System of Surgery, Ed. 1, London, John W. Parker and Son
1: 723, 1860
- [2] Stoll A. M. and Green L. C. The relationship between pain and tissue
damage due to thermal radiation. *Aviation Medical Acceleration Laboratory Reot.* 15 1958
- [3] von Meeh : Ober flächenmessungen des menschlichen Körpers. Ztschr.
Biol. 15: 435, 1879
- [4] Du Bois D., Du Bois E. F.:The measurment of the surface area of man.
A. M. A. Arch. Intern. Med. 15: 868-881, 1915
- [5] Berkow, S.: A method of estimating the extensiveness of lesions (burns
and scalds) based on surface area proportions. *Arch. Surg.* 8:138-148,
1924

- [6] Weidenfeld, S. Arch. Derm. Syph., Berlin, 61:33-56, 301-356, 1902
- [7] Lund, C., and Browder, N.: The estimation of areas of burns. *Surg. Gynec. & Obst.* 79:352-358, 1944.
- [8] Boyd, E. ;Growth of surface area of human body. *Minneapolis University of Minnesota Press*, 1935
- [9] Knaysi, G. A., Crikelair, G. F., Cosman, B.: The Rule of Nines :Its history and accuracy. *Plast. Rreconstr. Surg.* 41:560-563, 1968.
- [10] Nichter L. S., Bryant, C. A., Edlich,R. F.: Efficacy of burned surface area estimates calculated form charts–The need for a computer-based model”. *J. Trauma* 6: 477-481, 1985
- [11] Cole R.P., Jones S. G. and Shakespeare P. G.: Thermographic assessment of hand burns. *Burns* 16 :60-63, 1990
- [12] Ring E. F. J.:Thermal imaging and therapeutic drugs. *Prog. Clin. Biol. Res.*, 107: 463-474, 1982
- [13] Barnes R. B.:Thermography. *Ann. New York Acad Sc.* 121:34, 1964

- [14] Lawson, R. N.:Early applications of thermography. *Ann. New York Acad Sc.* 121:31, 1964
- [15] Brueschke, E. E.,Haberman, J. D. and Gershon-Cohen, J.Relative densitometric analysis of thermograms for more precise temperature determinations. *Ann. New York Acad Sc.* 121:80, 1964
- [16] Williams, K. L., Williams F. J. L. and Handley R. S. :Infrared thermometry in the diagnosis of breast disease. *Lancet* 2: 1378, 1961
- [17] Lawson R. N., Wlodek G. and Webster D. R. : Thermographic assessment of burns and frostbite. *Canad. M. A. J.* 84 :1129, 1961
- [18] Hackett M. E. J.: The use of thermography in the assessment of depth of burn and blood supply of flaps, with preliminary reports on its use in Dupuytren's contracture and treatment of varicose ulcers. *Br. J. Plast. Surg.* 27:311-317, 1974
- [19] Mehul M. Patel:320 \times 244 -Element PtSi SBD IR-CCD Camera system. *Master's Thesis, New Jersey Institute of Technology.* Aug. 1990

- [20] Steve Blume :Infrared TV Camera with PtSi Schottky- Barrier Detectors. *Master's Thesis, New Jersey Institute of Technology, Dec.* 1989
- [21] Wolfe W. L.:Infrard imaging devices in infrared medical radiography. *Ann. New York Acad Sc.* 121:57, 1964
- [22] Hardy, J. D.: The radiating power of human skin in the infra-red .*Am. J. Physiol.* 127:454, 1939
- [23] Gonzalez R.C.: Digital Image Processing. *Addison-Wesley Publishing Co.Inc.*, 1987
- [24] Plastock R. A. and Kalley G.: Theory and Problems of Computer Graphics. *McGraw-Hill,Inc.* 1986
- [25] Hearn D.and Baker M. P.:Computer Graphics. *Prentice-Hall international, Inc.* 1986
- [26] Jain A. K.: Fundamentals of Digital Image Processing. *Prentice-Hall internation, Inc.* 1989

- [27] Ballard D. H. and Brown C. M.: Computer Vision .*Prentice-Hall international Inc.* 1982
- [28] Schalkoff R. J.: Digital Image Processing and Computer Vision. *John Wiley & Sons Inc.* 1989
- [29] Hardy, J. D., Muschenheim, C.: The emission reflection and transmission of infra-red radiation by the human skin. *J. Clin. Invest.* 13:817, 1934
- [30] Mladick, R., Georgiade, N., Thorne, F.: A clinical evaluation of the use of thermography in determining degree of burn injury. *Plastic reconstr. Surg.* 38, 512-8 1966
- [31] Hackett, M.E.J. Colour thermography in the diagnosis of burn depth. Transactions of the Fifth International Congress in Plastic and Reconstructive Surgery. Butterworth, pp. 813-820 1971
- [32] Connel, J. F. and Morgan, E. and Rousselot, L. M.: Thermography in trauma. *Ann. New York Acad. Sc.* 121:172, 1964

- [33] Williams K. L.: Infrared thermometry as a tool in medical research. *Ann. New York Acad Sc.* 121:99, 1964
- [34] Atkins E.: Elevation of body temperature in disease. *Ann. New York Acad Sc.*, 121:26, 1964
- [35] Minard D., Copman L. and Dasler A. R.: Elevation of body temperature in health. *Ann. New York Acad Sc.* 121:12, 1964
- [36] Cade C. M.: High-speed thermography. *Ann. New York Acad. Sc.* 121:74, 1964
- [37] Dittmar A., Marich J., Grippari J. L., Delhomme G. and Roussel B.: Measurement by heat clearance of skin blood flow of healthy, burned, and grafted skin. *Progress Clin. Bio. Res.*, 107:413-419, 1982
- [38] Thomas D., Cullum D., Siahamis G. and Langlois S.: Infrared thermographic imaging, magnetic resonance imaging, catscan and myelography in low back pain. *Br. J. Rheumatol*, 29:268-273, 1990

- [39] Little R. A. and Stoner H. B.: Body temperature after accidental injury.
Br. J. Surg. 68 :221-224, 1981
- [40] IMAGE Program, Physiology Department, University of Medicine and
Dentistry of New Jersey, 1983
- [41] Leroy, Y.: Microwave radiometry and thermography-Present and
prospective. *Prog. Clin. Biol. Res.* 107:485-499, 1982

7 APPENDIX: BURN PROGRAM

FTN66

\$CDS ON

\$EMA /A/,/B/ ! revision: MAY.17.1991 by CHEN SHANG-YUAN

\$FILES 1,1

PROGRAM BURN

C The parameters are as follows:

C IARRY : workspace accessive for the user

C IPXL : reserved project space for picture processing

C LX,LY : actual line length,number of lines of the image
C residing in the workspace.

C LSX,LSY: starting address of the residing image

C LU,LQTX: Logic unit number of the terminal,Quantex,HP2240A
C ,I2240

C IFLAG, : represents the state of a Writefile

C IFLGR : " " " " " Readfile

C -1 : not yet logged on

C 0 : close open files

C 1 : no file open

C 2 : NF option was used; no files will be allowed

C > 10 : a file was created and is opened

C Note: all these parameters are global and passed via COMMON!

C JEQT,IEQT,IMENU are local dummy parameters.

C

C External subroutines: CONTR,FILER,LOGIN,PROC,MATH,QWRIT,TFMGR

C Calling procedure : RU,IMAGXX

C

C

C *****

C ** M A I N R O U T I N E **

C *****

```

C
C   This is the main routine of the program.
C   It initializes and guides the user through a mode menu.

```

```

C
C   INITIALIZATION

```

```

C
COMMON /A/ IARRY1(256,256),IARRY2(256,256),
+          JARRY1(256,256),JARRY2(256,256)
COMMON /B/ IBX(2000),IBY(2000),JBX(2000),JBY(2000)
COMMON LU,LQTX,ISC,JSC,LUBUS
COMMON /FLAG/IFLAG,IFLGR
COMMON /BUFR/ JBUF(128)
LU = LOGLU(LU)
LX1 = 0
LY1 = 0
LX2 = 0
LY2 = 0
IBELL = 3400B
ISWITCH = 0

```

C->The address of Quantex is set to 4! (Note in LBGET function)

```

LQTX = LBGET(LU,4,ISC,ISWITCH) ! ISWITCH = 0; RETURN SELECT CODE

```

```

C OF QUALIFYING DEVICE. ISWITCH = 1; FIND QUALIFYING DEVICE WHOSE
C SELECT CODE MATCHES ISC.

```

```

ISWITCH = 1
LUBUS = LBGET(LU,36B,ISC,ISWITCH)

```

```

IFLAG = -1
CALL LOGIN

```

```

10  WRITE (LU,12)
12  FORMAT(/////,17X,'*****'/,17X
1   '***  PROGRAM  IMAGE  ***'/,17X
2   '*****'/)

```

C->**** M A I N M E N U ****<-C

```

20  WRITE (LU,22) IBELL
22  FORMAT(A1)
    WRITE (LU,24)
24  FORMAT(///// '      IMAGE provides you a menu of basic functions: '//
1'      1. WRITE FIRST  FILE'//
2'      2. WRITE SECOND FILE'//
3'      3. WRITE THIRD  FILE'//
4'      4. WRITE FOURTH FILE'//
5'      5. BURNED SKIN PROCESSES'//
6'      6. AREA CALCULATION'//
7'      7. STOP the program'//
8'      Please type the number of the operation (1-7):  _')
    READ (LU,*,ERR=20) IMENU
    IF (IMENU.EQ.1) CALL QWRIT(IARRY1,LX1,LY1,LSX1,LSY1)
    IF (IMENU.EQ.2) CALL QWRIT(JARRY1,LX2,LY2,LSX2,LSY2)
    IF (IMENU.EQ.3) CALL QWRIT(IARRY2,LX1,LY1,LSX1,LSY1)
    IF (IMENU.EQ.4) CALL QWRIT(JARRY2,LX2,LY2,LSX2,LSY2)

    IF (IMENU.EQ.6) THEN
        CALL AREA2(IBX,IBY,IPT)
        CALL AREA2(JBX,JBY,JPT)
    ENDIF
    IF (IMENU.EQ.5) THEN
        WRITE(LU,*)'PLEASE INPUT THE FIRST PICTURE'

```

```

CALL FILER(1,IARRY1,LX1,LY1,LSX1,LSY1)
LSX1=1
LSY1=1
CALL WQTX(IARRY1,LX1,LY1,LSX1,LSY1)
WRITE(LU,*) 'PLEASE INPUT THE SECOND PICTURE'
CALL FILER(1,JARRY1,LX2,LY2,LSX2,LSY2)
LSX2=256
LSY2=1
CALL WQTX(JARRY1,LX2,LY2,LSX2,LSY2)
LSX3=1
LSY3=256
LSX4=256
LSY4=256
CALL BKWT(IARRY1,LX1,LY1,LSX3,LSY3,IARRY2)
CALL BKWT(JARRY1,LX2,LY2,LSX4,LSY4,JARRY2)
CALL BNDY(IARRY2,LX1,LY1,LSX3,LSY3,IBX,IBY,IPT)
CALL BNDY(JARRY2,LX2,LY2,LSX4,LSY4,JBX,JBY,JPT)
WRITE(LU,*) 'TRANSLATION AND ROTATION :-)' ...
CALL AXIS(IBX,IBY,IPT,I1,I2)
CALL AXIS(JBX,JBY,JPT,J1,J2)
MX=(IBX(I1)+IBX(I2))/2-(JBX(J1)+JBX(J2))/2
MY=(IBY(I1)+IBY(I2))/2-(JBY(J1)+JBY(J2))/2
CALL TRAN(JARRY2,LX2,LY2,MX,MY)
MX=(IBX(I1)+IBX(I2))/2
MY=(IBY(I1)+IBY(I2))/2
X1=REAL(IBX(I1))-IBX(I2)
Y1=REAL(IBY(I1))-IBY(I2)
X2=REAL(JBX(J1))-JBX(J2)
Y2=REAL(JBY(J1))-JBY(J2)
D1=SQRT(X1*X1+Y1*Y1)
D2=SQRT(X2*X2+Y2*Y2)
T=ACOS((X1*X2+Y1*Y2)/(D1*D2))

```

```

      CALL ROT(JARRY2,LX2,LY2,T,MX,MY)
      CALL WQTX(JARRY2,LX2,LY2,LSX4,LSY4)
      CALL COMBB(IARRY1,JARRY2,LX1,LY1)
      CALL WQTX(IARRY1,LX1,LY1,LSX1,LSY1)
ENDIF

```

```

C      READ(LU,*,ERR=20) ANG
C      CALL ROT(IARRY,LX1,LY1,ANG/180.0*3.1415,LX1/2,
C + LY1/2)
      IF (IMENU.EQ.7) GOTO 30

      GOTO 20

```

C->Ending sequence

```

30  WRITE (LU,32)
32  FORMAT(/" IMAGE:  Ending sequence begun . . .")
      IF (IFLAG.LT.10.AND.IFLGR.LT.10) GOTO 34
      IFLAG = 0
      CALL FILER(0,IARRY1,LX1,LY1,LSX1,LSY1)
      CALL FILER(0,JARRY1,LX2,LY2,LSX2,LSY2)
34  CALL LOGIN
      STOP 0001
      END

```

```

SUBROUTINE BKWT(KARRY, LX, LY, LSX, LSY, LARRY)
EMA KARRY,LARRY
DIMENSION KARRY(256,256), LARRY(256,256)
COMMON LU

```

```

5  WRITE(LU,*)'TELL ME THE THRESHOLDING VALUE 0(BLACK)-255(WHITE):'

```



```

READ(LU,*) IVAL

DO 20 I = 1,LX
DO 20 J = 1,LY
    IF (KARRY(I,J).LE.IVAL) THEN
        LARRY(I,J) = 0
    ELSE
        LARRY(I,J) = 255
    ENDIF
20 CONTINUE

CALL WQTX(LARRY,LX,LY,LSX,LSY)
WRITE(LU,*) 'DO YOU THINK IT IS GOOD? 0:bad, 1:good'
READ(LU,*) I
IF(I .NE. 1) GOTO 5

DO 10 I=1,LX
    LARRY(I,1)=255
10    LARRY(I,LY)=255
DO 15 I=1,LY
    LARRY(1,I)=255
15    LARRY(LX,I)=255

DO 40 I = 2, LX-1
DO 40 J = 2, LY-1
    MAX = 0
    IF (LARRY(I-1,J ) .EQ. 0) MAX = MAX + 1
    IF (LARRY(I-1,J-1) .EQ. 0) MAX = MAX + 1
    IF (LARRY(I-1,J+1) .EQ. 0) MAX = MAX + 1
    IF (LARRY(I ,J-1) .EQ. 0) MAX = MAX + 1
    IF (LARRY(I ,J+1) .EQ. 0) MAX = MAX + 1
    IF (LARRY(I+1,J-1) .EQ. 0) MAX = MAX + 1

```

```

        IF (LARRY(I+1,J ) .EQ. 0) MAX = MAX + 1
        IF (LARRY(I+1,J+1) .EQ. 0) MAX = MAX + 1
        IF (MAX .LT. 4) THEN
            LARRY(I,J) = 255
        ELSE IF (MAX .GT. 4) THEN
            LARRY(I,J) = 0
        ENDIF
40    CONTINUE
    CALL WQTX(LARRY,LX,LY,LSX,LSY)
    DO 45 I = 2,LX-1
    DO 45 J = 2,LY-1
        MAX = 0
        IF (LARRY(I-1,J-1) .EQ. 0) MAX = MAX + 1
        IF (LARRY(I-1,J ) .EQ. 0) MAX = MAX + 1
        IF (LARRY(I-1,J+1) .EQ. 0) MAX = MAX + 1
        IF (LARRY(I  ,J-1) .EQ. 0) MAX = MAX + 1
        IF (LARRY(I  ,J+1) .EQ. 0) MAX = MAX + 1
        IF (LARRY(I+1,J-1) .EQ. 0) MAX = MAX + 1
        IF (LARRY(I+1,J ) .EQ. 0) MAX = MAX + 1
        IF (LARRY(I+1,J+1) .EQ. 0) MAX = MAX + 1
        IF (MAX .LT.4) THEN
            LARRY(I,J) = 255
        ELSE IF (MAX .GT. 4) THEN
            LARRY(I,J) = 0
        ENDIF
45    CONTINUE
    CALL WQTX(LARRY,LX,LY,LSX,LSY)
    RETURN
END

SUBROUTINE BNDY(KARRY,LX,LY,LSX,LSY,KBX,KBY,NPT)
    EMA KARRY,KBX,KBY

```

```

COMMON LU
DIMENSION KARRY(256,256),KBX(2000),KBY(2000)

5  WRITE(LU,*)'TELL ME A POINT LOCATING IN THE BOUNDARY (X,Y):'
   READ(LU,*) INITY,INITX
   IF(KARRY(INITX,INITY) .EQ. 255) GOTO 5

   KARRY(INITX,LY) = 255
10  IF (KARRY(INITX,INITY+1) .EQ. 0) THEN
      INITY = INITY + 1
      GOTO 10
   END IF

   NPT = 0
   IDIR = 0
   I = INITX
   J = INITY
70  NPT = NPT + 1
      KBX(NPT) = I
      KBY(NPT) = J

75  IDIR = IDIR + 1
      IF (IDIR .EQ. 8) IDIR = 0
      IF (IDIR .EQ. 0) THEN
          IF (KARRY(I ,J+1) .EQ. 0) THEN
              J = J + 1
              IDIR = 4
              GOTO 80
          ENDIF
      ELSE IF (IDIR .EQ. 1) THEN
          IF (KARRY(I+1,J+1) .EQ. 0) THEN
              I = I + 1

```

```

        J = J + 1
        IDIR = 5
        GOTO 80
    ENDIF
ELSE IF(IDIR .EQ. 2) THEN
    IF (KARRY(I+1,J ) .EQ. 0) THEN
        I = I + 1
        IDIR = 6
        GOTO 80
    ENDIF
ELSE IF(IDIR .EQ. 3) THEN
    IF (KARRY(I+1,J-1) .EQ. 0) THEN
        I = I + 1
        J = J - 1
        IDIR = 7
        GOTO 80
    ENDIF
ELSE IF(IDIR .EQ. 4) THEN
    IF (KARRY(I ,J-1) .EQ. 0) THEN
        J = J - 1
        IDIR = 0
        GOTO 80
    ENDIF
ELSE IF(IDIR .EQ. 5) THEN
    IF (KARRY(I-1,J-1) .EQ. 0) THEN
        I = I - 1
        J = J - 1
        IDIR = 1
        GOTO 80
    ENDIF
ELSE IF(IDIR .EQ. 6) THEN
    IF (KARRY(I-1,J ) .EQ. 0) THEN

```

```

        I = I - 1
        IDIR = 2
        GOTO 80
    ENDIF
ELSE IF(IDIR .EQ. 7) THEN
    IF (KARRY(I-1,J+1) .EQ. 0) THEN
        I = I - 1
        J = J + 1
        IDIR = 3
        GOTO 80
    ENDIF
ENDIF
GOTO 75
80  IF ((I .NE. INITX) .OR. (J .NE. INITY)) GOTO 70

    NPT = NPT + 1
    KBX(NPT)=KBX(1)
    KBY(NPT)=KBY(1)

    DO 79 I = 1, LX
    DO 79 J = 1, LY
79      KARRY(I,J) = 255

    DO 89 I = 1, NPT
89      KARRY(KBX(I),KBY(I)) = 0

    CALL WQTX(KARRY,LX,LY,LSX,LSY)

    RETURN
    END

    SUBROUTINE TRAN(KARRY, LX, LY, H, K)

```

```

      EMA KARRY,ITEMP
      COMMON LU
      DIMENSION KARRY(256,256), ITEMP(256,256)
      INTEGER H,K

      DO 10 I = 1, LX
      DO 10 J = 1, LY
          IX = I - H
          IY = J - K
          IF(IX.LT.1 .OR. IX.GT.LX .OR. IY.LT.1 .OR. IY.GT.LY) THEN
              ITEMP(I,J)=255
          ELSE
              ITEMP(I,J)=KARRY(IX,IY)
          ENDIF
10      CONTINUE
      DO 20 I=1,LX
      DO 20 J=1,LY
20      KARRY(I,J)=ITEMP(I,J)
      RETURN
      END

```

```

SUBROUTINE ROT(KARRY, LX, LY, THETA, H, K)
      EMA KARRY,ITEMP
      COMMON LU
      DIMENSION KARRY(256,256), ITEMP(256,256)
      INTEGER H,K
      REAL THETA

```

```

      SIN THE = SIN(0.0 - THETA)
      COS THE = COS(0.0 - THETA)

```

```

      T1 = -1.0 * H * COS THE + K * SIN THE + H

```

```

T2 = -1.0 * H * SIN THE - K * COSTHE + K
DO 10 IY = 1, LY
DO 10 IX = 1, LX
    X = IX * COSTHE - IY * SIN THE + T1
    Y = IX * SIN THE + IY * COSTHE + T2
    IF ((X .LE. 1.) .OR. (X .GE. LX-1.) .OR.
+      (Y .LE. 1.) .OR. (Y .GE. LY-1.)) THEN
        ITEMP(IX,IY) = 255
    ELSE
        ALFA = X - INT(X)
        BETA = Y - INT(Y)
        I = INT(X)
        J = INT(Y)
        ITEMP(IX,IY)=INT((1.0 - ALFA)*(1.0 - BETA)*KARRY(I ,J )+
1          (1.0 - ALFA)*      BETA *KARRY(I ,J+1)+
2          (      ALFA)*(1.0 - BETA)*KARRY(I+1,J )+
3          (      ALFA)*      BETA *KARRY(I+1,J+1))
        ENDIF
10    CONTINUE
    DO 20 IY = 1, LX
    DO 20 IX = 1, LY
        KARRY(IX, IY) = ITEMP(IX, IY)
20    CONTINUE
    RETURN
    END

```

```

SUBROUTINE COMBB(KARRY,LARRY,LX,LY)
    EMA KARRY,LARRY
    DIMENSION KARRY(256,256),LARRY(256,256)
    DO 10 I=1,LX
    DO 10 J=1,LY
        IF(LARRY(I,J).GT.128)THEN

```

```

        LARRY(I,J)=255
    ELSE
        LARRY(I,J)=0
    ENDIF
    IF(LARRY(I,J).LT.KARRY(I,J)) THEN
        KARRY(I,J)=LARRY(I,J)
    ENDIF
10  CONTINUE
    RETURN
    END

SUBROUTINE AREA1(KARRY,LX,LY)
    EMA KARRY
    COMMON LU
    DIMENSION KARRY(256,256)
    ICOUNT=0
    DO 10 I=1,LX
    DO 10 J=1,LY
        IF(KARRY(I,J).EQ.0) ICOUNT=ICOUNT+1
10  CONTINUE
    WRITE(LU,*) 'AREA1=', ICOUNT
    RETURN
    END

SUBROUTINE AREA2(KBX,KBY,NPT)
    EMA KBX,KBY
    COMMON LU
    DIMENSION KBX(2000),KBY(2000)

    WRITE(LU,*) 'TELL ME 1 PIXEL=? CM X CM'
    READ(LU,*) PIX
    SUM=0

```



```

DO 10 I=1,NPT-1
    SUM=SUM+(KBY(I)+KBY(I+1))*(KBX(I)-KBX(I+1))
10  CONTINUE
    SUM=SUM/2
    WRITE(LU,*) 'AREA= ',ABS(SUM*PIX)
    RETURN
END

```

```

SUBROUTINE AXIS(KX,KY,NPT,I1,I2)
COMMON LU
EMA KX,KY
DIMENSION KX(2000),KY(2000)
DMAX=0.0
DO 10 I=1,NPT-1
DO 10 J=I+1,NPT-1
DIS=REAL((KX(I)-KX(J))*(KX(I)-KX(J))+
+ REAL((KY(I)-KY(J))*(KY(I)-KY(J))
IF (DIS.GT.DMAX) THEN
    DMAX=DIS
    I1=I
    I2=J
ENDIF
10  CONTINUE
RETURN
END

```

```

FUNCTION LBGET(LU,IAD,KSC,ISWITCH)
C ----- -- ---
C->Loop to search for QUANTEX bus number

```

```

DO 10,LLU=7,63
LBGET = LLU

```

```

CALL EXEC(100015B,LLU,I,J,K) ! The no-abort option is used here
GOTO 10                       ! This line is executed on error

```

C->Logical match and fooling the compiler

```

2      IF (IAND(J,37400B).EQ.17400B.AND.IAND(K,37B).EQ.IAD)THEN
          IF(ISWITCH.EQ.0)THEN
              KSC=IAND(J,77B)
              RETURN
          ELSE
              IF(KSC.EQ.IAND(J,77B))RETURN
          ENDIF
      ENDIF
10     CONTINUE
      LBGET = 0

```

C->Error message

```

      WRITE (LU,12) IAD
12     FORMAT(" LU address "I2," cannot be computed on this bus!")
      RETURN
      END

```

C

C

C *****

C ** SUBROUTINE QWRIT **

C *****

C

C ...is a control unit for most output functions.

C

```

      SUBROUTINE QWRIT(KARRY,LX,LY,LSX,LSY)

```

C -----

```

EMA KARRY
COMMON LU,LQTX,ISC,JSC,LUBUS
DIMENSION KARRY(256,256)
IBELL = 3400B
IF (LX.GT.0) GOTO 3333
IF (LX.EQ.0) WRITE (LU,14) IBELL
14  FORMAT(A1,"There æ&dDisn'tæ&d@ any data in the program's memory!")
RETURN

```

```

3333 WRITE (LU,42)
42  FORMAT(//' Now we have something to write!'/
1  ' Select one of the following possibilities: '//
2  '   1. Write the image beginning at the predefined location.'/
3  '   2. Write the image into a defined window.'/
5  '   4. Store the image in a file.'/
7  '   6. Go back to menu.          _'//)
READ (LU,*,ERR=3333) ISELC
IF (ISELC.LT.1.OR.ISELC.GT.6) GOTO 3333
IF (ISELC.EQ.1) CALL WQTX(KARRY,LX,LY,LSX,LSY)
IF (ISELC.EQ.2) CALL WINDW(KARRY,LX,LY,LSX,LSY)
IF (ISELC.EQ.4) CALL FILER(0,KARRY,LX,LY,LSX,LSY)
IF (ISELC.EQ.4.OR.ISELC.EQ.5) GOTO 3333
RETURN
END

```

```

C
C *****
C **  SUBROUTINE  W Q T X      **
C *****
C
C Write to Quantex memory

```

```

C ...initializes the Quantex for write procedures.
C
C   It sets up the outputstring in Quantex "NIBBLE" format
C   then it puts out the dimensioned IARRY.
C
      SUBROUTINE WQTX(KARRY,LX,LY,LSX,LSY)
C   -----
C
      EMA KARRY
      COMMON LU,LQTX,ISC,JSC,LUBUS
      DIMENSION NPL(5),INTO(5),ITEMP(128),KARRY(256,256)
C
C->Convert the workspace into a compressed output field
C and set up the address string.

      CALL COMB(KARRY,LX,LY,LSX,LSY)
      ICLMN = LSX
      JROW = LSY
      NLX=INT((LX+1)/2.)
      DO 10 J=1,LY
      IROW = JROW + J - 1
      CALL ADRCV(IROW,ICLMN,NPL)
      INTO(1) = 00461B
      INTO(2) = 21002B
      INTO(3) = IOR (( ISHFT (NPL(1),8)) , NPL(2))
      INTO(4) = IOR (( ISHFT (NPL(3),8)) , NPL(4))
      INTO(5) = IOR (( ISHFT (NPL(5),8)) , 0017B)
C
      DO 5 J1=1,LX,2
      JJ=INT((J1+1)/2.)
      ITEMP(JJ)=KARRY(J,J1)
5    CONTINUE

```

```

C
C->EXEC will cause a Interface Clear -) the only way
C  to get Quantex attention!
C
      CALL EXEC(3,LUBUS+5100B)
      CALL EXEC(2,LQTX+2100B,INT0,5)
10   CALL EXEC(2,LQTX+2100B,ITEMP,NLX)
      CALL SEPAR(KARRY,LX,LY,LSX,LSY)
      RETURN
      END
C
C *****
C ** SUBROUTINE  W I N D W **
C *****
C
C Description:
C window replaces the dormant workspace to any defined
C position in the memory(==screen).
C
      SUBROUTINE WINDW(KARRY,LX,LY,LSX,LSY)
C -----
C
      EMA KARRY
      COMMON LU
      DIMENSION KARRY(256,256)

C->Store the original window

      ISLX = LX
      ISLY = LY
      ISLSX = LSX
      ISLSY = LSY

```

C->Dialog, and do the window

```
10  WRITE (LU,12)
12  FORMAT(" Type your new start address (column,row)? _")
    READ (LU,*,ERR=10) LSX,LSY
    IF (LSX.EQ.1000) RETURN
    IF (LSX.GT.512.OR.LSY.GT.512) GOTO 10
20  WRITE (LU,22)
22  FORMAT(" Type length of field (x,y)? _")
    READ (LU,*,ERR=20) LX,LY
    IF (LX.GT.256.OR.LY.GT.256) GOTO 20
    CALL WQTX(KARRY,LX,LY,LSX,LSY)
    WRITE (LU,24)
24  FORMAT(" Would you like to save this image? _")
    READ (LU,26) IANSW
26  FORMAT(A1)
    IF (IANSW.EQ.1HY) CALL FILER(0,KARRY,LX,LY,LSX,LSY)
```

C->Restore the original window

```
LX = ISLX
LY = ISLY
LSX = ISLSX
LSY = ISLSY
RETURN
END
```

```
C  *****
C  ** SUBROUTINE  L O G I N  **
C  *****
C
```

```

        SUBROUTINE LOGIN
C      -----

C
C->This subroutine,'LOGIN', just prints a header and a closing
C statement on logging off.
C
        COMMON LU
        COMMON /FLAG/IFLAG,IFLGR
        IF (IFLAG.EQ.-1) GOTO 30

C->Logging off

        WRITE (LU,2)
2      FORMAT(" IMAGE:  Logging off now . . . bye!"/)
        RETURN

C->Logging on

30     WRITE (LU,32)
32     FORMAT(////////" IMAGE:  A data acquisition and processing program"/
1" servicing the Quantex digital image memory in communication "/
2" with the Hewlett-Packard 1000 computer system."///)
        CALL EXEC(12,0,2,0,-1) ! wait 1 sec, then continue
        IFLAG = 1
        IFLGR = 1
        RETURN
        END

C
C      *****
C      ** SUBROUTINE  A D R C V      **
C      *****

```

```

C      SUBROUTINE ADRCV(IRW,ICLMN,NPL)
C      -----
C
C      Address Conversion takes a given row and column, and cal-
C      calculates the Quantex memory address or pixelcount.
C      As output a array in nibble QUANTEX format is provided.
C
C      Remark: the Quantex memory has a 18 Bit address. Since we
C      are working on a 16 Bit integer base we prevent overflow
C      by dividing the row into blocks of 128 lines.
C      If the row number is >512 the program will print a error-
C      message and terminate the program!
C      Input  : IRW,ICLMN
C      Output : NPL(1-5)
C
COMMON LU
COMMON /FLAG/IFLAG,IFLGR
DIMENSION NPL(5)
IROW = IRW
DO 10,I=1,4
  J = I-1
  IF (IROW.LE.128) I = 4
  IROW = IROW - 128
10  CONTINUE
  NPL(5) = J + 000140B
  IROW = IROW + 128
  IF (IROW.LE.128) GOTO 20
  WRITE (LU,12)
12  FORMAT("Row too big!!!")
  IFLAG = 0
  CALL LOGIN

```


C->Calculate the 16 Bit address and combine the 4 Bit data with
C 4 Bit Quantex control data (2-6).

```

20  IF (IROW.EQ.0) IROW = 1
    IADR = ((IROW-1) * 512) + ICLMN
    ISHRG = IADR
    DO 30 I=1,4
      J = I + 1
      NPL(I) = IAND (ISHRG,017B)
      JJ = ISHFT(J,4)
      NPL(I) = IOR (NPL(I),JJ)
      ISHRG = IADR
      ISHRG = ISHFT (ISHRG,-4)
      IADR = ISHRG
30  CONTINUE
    RETURN
    END

```

```

C
C *****
C ** SUBROUTINE COMBINE **
C *****
C
C combines 2 adjacent integers in a 16 bit word (2n-1 spaced)
C
C   Input  : IARRAY containing 0 to 255 integers
C   Output : IARRAY with compressed contents.
C
C
C SUBROUTINE COMB(KARRAY,LX,LY,LSX,LSY)
C -----
C   EMA KARRAY
C   DIMENSION KARRAY(256,256)

```

```

DO 111 I=1,LY
DO 111 J=1,LX
J1 = J+1
111 KARRY(I,J) = IOR (ISHFT (KARRY(I,J),8) , KARRY(I,J1))
RETURN
END

C
C *****
C ** SUBROUTINE SEPARATE **
C *****
C
C Separates the two compressed pixelintegers (16 bit)
C
C Input : IARRY containing a 2*8bit information in the
C         (2n-1) field location.
C Output : IARRY containing 0 to 255 integers.
C
C
C SUBROUTINE SEPAR(KARRY,LX,LY,LSX,LSY)
C -----
C EMA KARRY
C DIMENSION KARRY(256,256)
C DO 111 I=1,LY
C DO 111 J=1,LX,2
C ISAVE = KARRY(I,J)
C J1 = J+1
C KARRY(I,J) = ISHFT (KARRY(I,J) , -8)
C KARRY(I,J1) = IAND (ISAVE,0377B)
111 CONTINUE
RETURN
END

C *****

```

```

C      ** SUBROUTINE  F I L E R      **
C      *****
C
C      Description:
C      does all filehandling in a dialog mode. It keeps track of
C      opened files with FLAG and IFLGR, and allows only one open
C      file at a time.
C
C      A data compression is done to save memory(see COMB).
C      call proc. : CALL FILER(IRQST,IARRY)  &  COMMON's
C
C      SUBROUTINE FILER(IRQST,KARRY,LX,LY,LSX,LSY)
C      -----
C
C      EMA KARRY
C      COMMON LU
C      COMMON /FLAG/IFLAG,IFLGR
C      COMMON /BUFR/JBUF(128)
C      DIMENSION INBUF(64),KARRY(256,256),JTIME(15),LBUF(128)
C      DIMENSION IHEAD(16),ITIME(5)
C      DATA IHEAD/16*1H /
C      CALL LGBUF(JBUF,128)

```

C->control to read or write sections

```

      IF (IRQST.EQ.1) GOTO 500

```

C->write section

```

      IF (IFLGR.GT.10) CLOSE (88,IOSTAT=IERR,ERR=999,STATUS='KE')
      IF (IFLAG.GT.10) GOTO 100  ! file is already open,ready to be written
      IF (IFLAG.EQ.0) GOTO 200  ! file needs to be closed

```

C->dialog with loser

```
        IFLAG = IFLAG + 10
        WRITE (LU,4)
4       FORMAT("/Please input file namr:  _")
        READ (LU,6) (INBUF(I),I=1,64)
6       FORMAT(64A2)
```

C->open file

```
        OPEN(88,IOSTAT=IERR,ERR=999,FILE=INBUF,STATUS='UN')
```

C->puts header on file

```
        WRITE (88,10,IOSTAT=IERR,ERR=999)
10      FORMAT(1X,10HIMAGE FILE)
        CALL FTIME(JTIME)
        WRITE (88,12,IOSTAT=IERR,ERR=999) (JTIME(I),I=1,15)
12     FORMAT(15A2)
```

C->get system time; store msec with size of image

```
        CALL EXEC(11,ITIME)
100     ENCODE(32,102,IHEAD) ITIME(2),LX,LY,LSX,LSY
102     FORMAT(5I4)
        WRITE (88,104,IOSTAT=IERR,ERR=999) (IHEAD(I),I=1,16)
104     FORMAT(16A2)
        WRITE (LU,106)
106     FORMAT("/IMAGE:  parameters written to file"/)
```

C->compress data; write to file one line at a time

```

      CALL COMB(KARRY,LX,LY,LSX,LSY)
      IFLAG = 11
      NEWLX = (LX + 1) / 2
      DO 110 I=1,LY
      DO 108 J=1,LX,2
108   LBUF((J + 1) / 2) = KARRY(I,J)
110   WRITE (88,112,IOSTAT=IERR,ERR=999) (LBUF(K),K=1,NEWLX)
112   FORMAT(128A2)
      WRITE (LU,114)
114   FORMAT("/IMAGE:  data written to file  "/)

```

C->separate data

```

      CALL SEPAR(KARRY,LX,LY,LSX,LSY)

```

C->close file

```

200   CLOSE(88,IOSTAT=IERR,ERR=999,STATUS='KE')
      WRITE (LU,202)
202   FORMAT("/IMAGE:  file closed successfully"/)
      IF (IFLAG.GT.10) IFLAG = IFLAG-10
      IF (IFLGR.GT.10) IFLGR = IFLGR-10
      RETURN

```

C->READ SECTION

C ---- -

```

500   IF (IFLAG.GT.10) CLOSE(88,IOSTAT=IERR,ERR=999,STATUS='KE')
      IF (IFLGR.GT.10) GOTO 600 !  file is open already
      IF (IFLAG.EQ.0) GOTO 200 !  close up & get out

```

C->open file

```
IFLGR = IFLGR+10
READ (LU,6) (INBUF(I),I=1,64)
OPEN (88,IOSTAT=IERR,ERR=999,FILE=INBUF,STATUS='OL')
```

C->read header

```
600 READ (88,602,IOSTAT=IERR,ERR=999) (IHEAD(I),I=1,16)
602 FORMAT(16A2)
WRITE (LU,602) (IHEAD(I),I=1,16)
READ (88,602) (IHEAD(I),I=1,16)
WRITE (LU,602) (IHEAD(I),I=1,16)
```

C->assign file data to LX,LY,etc.

```
READ (88,604,IOSTAT=IERR,ERR=999) (IHEAD(I),I=1,10)
604 FORMAT(10A2)
DECODE (32,606,IHEAD) ITIME(2),LX,LY,LSX,LSY
606 FORMAT(5I4)
```

C->read file data

```
NEWLX = (LX + 1) / 2
DO 610 I=1,LY
READ (88,112,IOSTAT=IERR,ERR=999) (LBUF(J),J=1,NEWLX)
DO 608 J=1,LX,2
608 KARRY(I,J) = JBUF((J + 1) / 2)
610 CONTINUE
```

C->separate workspace

```

        CALL SEPAR(KARRY,LX,LY,LSX,LSY)
        WRITE (LU,612)
612    FORMAT(/"IMAGE:  file read successfully"/)
        GOTO 200

```

C->if error occurs, call FIERR routine

```

999    CALL FIERR(IERR)
        RETURN
        END

```

```

C*****
C*      SUBROUTINE FIERR(IERR)          *
C*****
        SUBROUTINE FIERR(IERR)
C      -----
        COMMON LU

        IF (IERR.EQ.462.OR.IERR.EQ.506) THEN
            WRITE (LU,10)
        ELSE IF (IERR.EQ.459.OR.IERR.EQ.508) THEN
            WRITE (LU,11)
        ELSE IF (IERR.EQ.502) THEN
            WRITE (LU,12)
        ELSE IF (IERR.EQ.507) THEN
            WRITE (LU,13)
        ELSE IF (IERR.EQ.514) THEN
            WRITE (LU,14)
        ELSE IF (IERR.EQ.515) THEN
            WRITE (LU,15)
        ELSE IF (IERR.EQ.532) THEN
            WRITE (LU,16)

```

```

ELSE IF (IERR.EQ.533) THEN
    WRITE (LU,17)
ELSE IF (IERR.EQ.546) THEN
    WRITE (LU,18)
ELSE
    WRITE (LU,19) IERR
ENDIF

10  FORMAT("/IMAGE: File not found")
11  FORMAT("/IMAGE: File already open")
12  FORMAT("/IMAGE: Duplicate file name")
13  FORMAT("/IMAGE: Wrong security code")
14  FORMAT("/IMAGE: Directory full")
15  FORMAT("/IMAGE: Illegal file name")
16  FORMAT("/IMAGE: Cartridge not found - probably not mounted")
17  FORMAT("/IMAGE: No room on cartridge")
18  FORMAT("/IMAGE: File has too many extents")
19  FORMAT("/IMAGE: File handling error "I3," occured.")

    WRITE (LU,100)
100  FORMAT("/Would you like to continue with the program,"/
1"or stop here?  _")
102  READ (LU,104) IANS
104  FORMAT(A1)
    IF (IANS.EQ.1HC) RETURN
    IF (IANS.NE.1HS) THEN
        WRITE (LU,106)
106  FORMAT("/Please answer with a C or S  _")
        GOTO 102
    ENDIF

IFLAG = 0

```


CALL LOGIN
STOP 0005
END